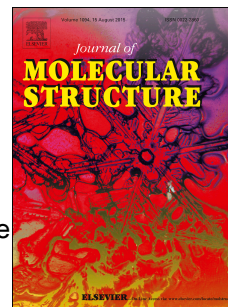


# Accepted Manuscript

Syntheses, spectroscopic characterization, SOD-like properties and antibacterial activities of dimer copper (II) and nickel (II) complexes based on imine ligands containing 2-aminothiophenol moiety: X-ray crystal structure determination of disulfide Schiff bases



Sulakshna Bharti, Mukesh Choudhary, Bharti Mohan, S.P. Rawat, S.R. Sharma, K. Ahmad

PII: S0022-2860(18)30330-2

DOI: [10.1016/j.molstruc.2018.03.041](https://doi.org/10.1016/j.molstruc.2018.03.041)

Reference: MOLSTR 24980

To appear in: *Journal of Molecular Structure*

Received Date: 18 September 2017

Revised Date: 8 March 2018

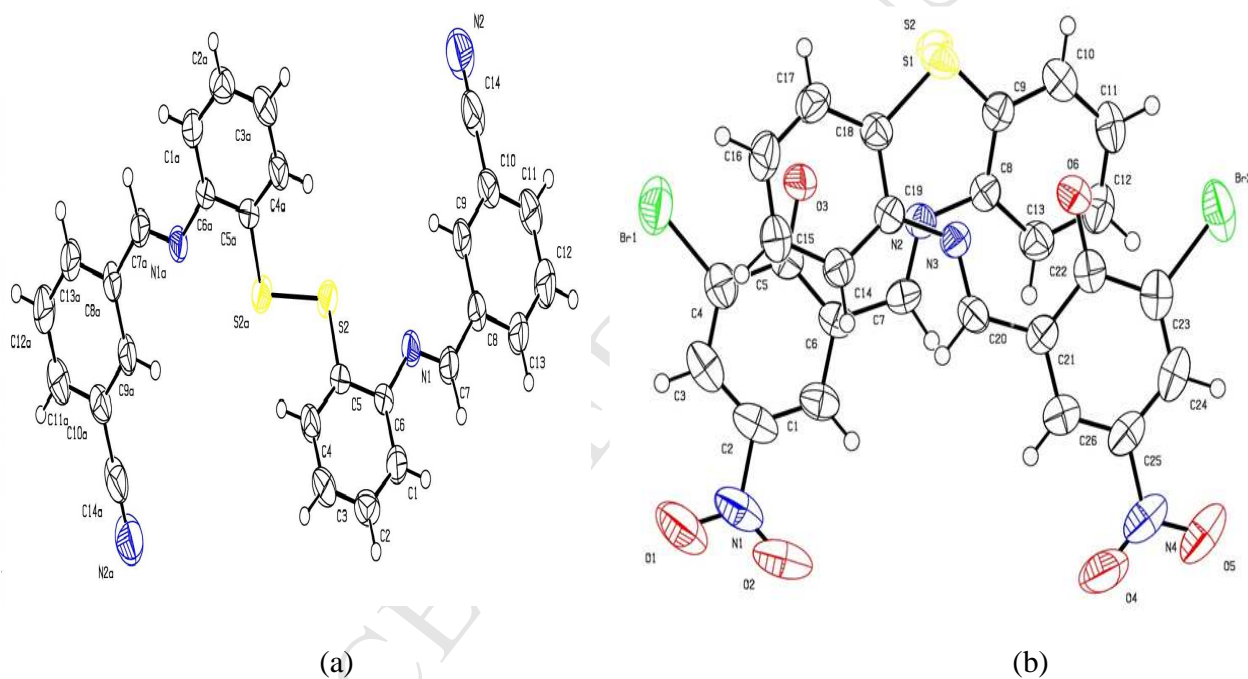
Accepted Date: 12 March 2018

Please cite this article as: S. Bharti, M. Choudhary, B. Mohan, S.P. Rawat, S.R. Sharma, K. Ahmad, Syntheses, spectroscopic characterization, SOD-like properties and antibacterial activities of dimer copper (II) and nickel (II) complexes based on imine ligands containing 2-aminothiophenol moiety: X-ray crystal structure determination of disulfide Schiff bases, *Journal of Molecular Structure* (2018), doi: 10.1016/j.molstruc.2018.03.041.

This is a PDF file of an unedited manuscript that has been accepted for publication. As a service to our customers we are providing this early version of the manuscript. The manuscript will undergo copyediting, typesetting, and review of the resulting proof before it is published in its final form. Please note that during the production process errors may be discovered which could affect the content, and all legal disclaimers that apply to the journal pertain.

**Graphical Abstract:**

Three new dimer complexes of copper (II) and nickel (II) were designed and successfully synthesized using the Schiff base ligands which was formed by the condensation of 2-aminothiophenol with 2-methoxybenzaldehyde, 3-formylbenzonitrile and 3-bromo-2-hydroxy-5-nitrobenzaldehyde, respectively. The main idea of this paper is the synthesis, characterization and catalytic activity of SOD-like metallic complexes. All the synthesized metal complexes are found to be binuclear and confirmed by elemental analyses, magnetic susceptibility measurements and ESR spectroscopy. The X-ray structures of the Schiff base ligands showed that in the crystalline form the SH groups were oxidized to produce a disulfide Schiff bases as a new double Schiff base ligands (Fig. 1(a) and 1(b)).

**Fig. 1(a) and 1(b).**

## Syntheses, spectroscopic characterization, SOD-like properties and antibacterial activities of dimer copper (II) and nickel (II) complexes based on imine ligands containing 2-aminothiophenol moiety: X-ray crystal structure determination of disulfide Schiff bases

Sulakshna Bharti<sup>a</sup>, Mukesh Choudhary<sup>a\*</sup>, Bharti Mohan<sup>a</sup>, S. P. Rawat<sup>b</sup>, S. R. Sharma<sup>a</sup> and K. Ahmad<sup>a</sup>

<sup>a</sup>Department of Chemistry, National Institute of Technology Patna, Ashok Raj path, Patna -800005, Bihar, India.

<sup>b</sup>Department of Chemistry, Govt. Vivekanand P. G. College, Maihar-485 771, Madhya Pradesh, India.

\*Corresponding author: mukesh@nitp.ac.in

### Abstract:

A series of new dimer complexes of copper (II) and nickel (II) were designed and synthesized using the Schiff base ligands which was formed by the condensation of 2-aminothiophenol with 2-methoxybenzaldehyde, 3-formylbenzonitrile and 3-bromo-2-hydroxy-5-nitrobenzaldehyde, respectively. The **synthesized metallic complexes** were characterized by using different physicochemical and spectroscopic methods. The most plausible geometry for the 1:2 complexes appeared to be distorted square-planar or tetrahedral environments. All the synthesized metal complexes are found to be binuclear and confirmed by elemental analyses, magnetic susceptibility measurements and ESR spectroscopy. The Schiff base ligands ( $HL^1/HL^2/H_2L$ ) were coordinated to the metal ions through the ONS/SNN and / or **N, S donor** atoms. In order to prevent the oxidation of the thiol group during the formation of Schiff bases and its complexes, all of the reactions were carried out under an inert atmosphere of argon. The X-ray structures of the Schiff base ligands showed that in the crystalline form the SH groups were oxidized to produce a disulfide Schiff bases as a new double Schiff base ligands ( $L^1_a/L^2_a/H_2L_a$ ). The  $L^1_b$  ligand is a bicyclic ring system of N, S-containing heterocyclic. The crystal structures of the double Schiff bases were determined by single crystal X-ray diffraction. The molar conductivity values of the complexes in DMSO implied the presence of non-electrolyte species. The SOD-like activity of Schiff bases and its complexes were investigated by NBT-DMSO assay and IC<sub>50</sub> values were evaluated. Their biological properties have also been studied. These complexes were also tested for their *in vitro* antibacterial screening activities against three bacteria (*Streptococcus aureus*, *Salmonella typhi*, and *Escherichia coli*) comparing with the Schiff base ligands. Most of the complexes have higher antibacterial activities than those of the free Schiff bases, **double Schiff bases** and the control.

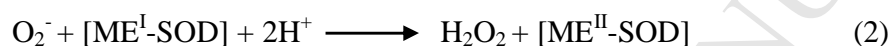
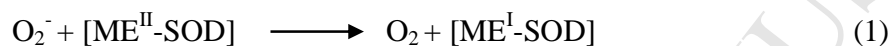
**Keywords:** Dimer copper (II) and nickel (II) complexes; 2-aminothiophenol moiety; crystal structures of disulfide Schiff bases; catalytic SOD-like properties; Antibacterial screening activities.

## 1. Introduction

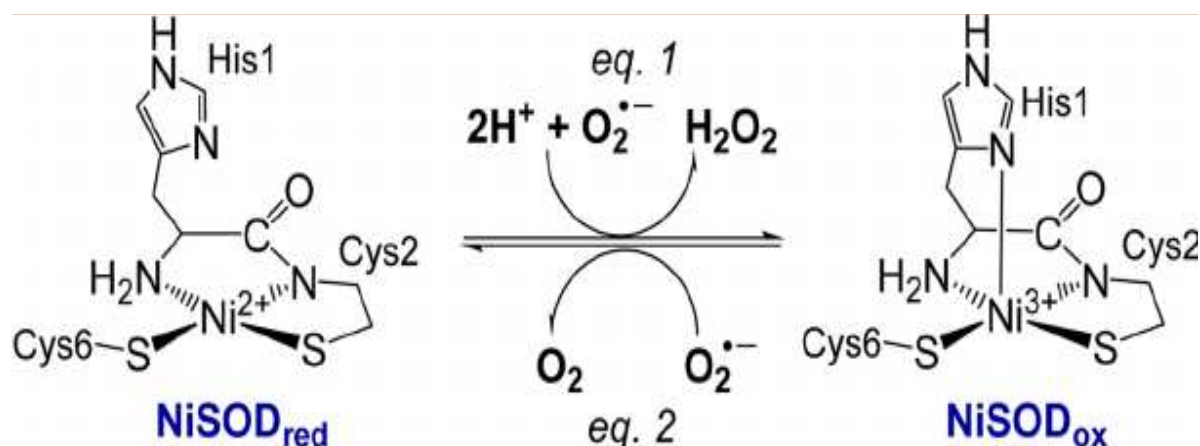
The thiazole units are found in many naturally occurring compounds [1]. Benzothiazoles are used as neuroprotectors [2] and antioxidants [3]. It consists of a five-membered 1, 3-thiazole ring fused to a benzene ring [4]. Metal complexes with 2-(2-methoxyphenyl) benzo[*d*]thiazole as N and S chelating ligands have attracted considerable attention because of their interesting physicochemical properties and pronounced biological and pharmacological activities [5-7]. Schiff bases are an important class of organic compounds [8]. This kind of ligands have significant importance in chemistry, especially in the development of Schiff base complexes because Schiff base ligands are potentially capable of forming stable complexes with metal ions [9]. Schiff base ligands with N and S donor atoms in their structures act as good chelating agent for metal ions [10]. The N and S atoms play a key role in the coordination of metals at the active sites of various metallo-biomolecules. Coordination of such compounds with metal ions, such as copper, nickel and iron often enhance their biological activities [11, 12]. Schiff base ligands have proven to be very effective in constructing supramolecular architectures such as coordination polymers, double helices and triple helicates [13]. These complexes have significant contribution in the development of catalysis and enzymatic reactions, magnetism, molecular architectures and materials chemistry [13, 14]. Schiff base metal complexes have been interest in coordination chemistry for many years due to their facile synthesis and wide applications. Interest in coordination chemistry of tridentate Schiff base ligands with **N, O and S** donating sites have increased due to the capabilities of forming stable complexes of four, five or six coordinated [15,16] and have a broad range of antifungal [17], antibacterial [18] anticancer [19] properties. **Particular attention has been devoted to tridentate ONS donor Schiff base ligands containing 2-aminothiophenol moiety because they can promote chelation and provides extra stability to the metal centres** in its 1:1 and/or 1:2 complexes. In all complexes, the Schiff base ligands either behave as tridentate (ONS/SNN) and/or bidentate-N, S donor ligands. The most plausible geometry for the 1:2 complexes appeared to be a distorted square planar (four coordinated) or tetrahedral.

**Superoxide dismutase is an important antioxidant to control the free radical reactions related to superoxide generated in biological system [20]. However, its large molecule and short life span *in vivo* limit its clinical use. Extensive studies have been carried out to find the suitable SOD-mimics to substitute it. In order to acts as SOD mimics, a compound should be non-toxic, stable, and easy to reach its targets and retain high SOD activity *in vivo*.** Synthetic transition metal complexes mimicking superoxide dismutase, provide models for metalloproteins active sites and lend inside towards the design of new catalysis. Metal complexes with Schiff base ligands behave as better catalysts for Cu, Zn-SOD enzyme [21, 22]. This metalloenzyme is a dimeric protein with two identical subunits each containing one Cu (II) and Zn (II). X-ray crystallographic studies [23] have shown that the Cu (II) and Zn (II) ions exist in distorted

square planar and tetrahedral coordination environments, respectively. Superoxide dismutase (SOD) is dedicated to keep the concentration of  $O_2^-$  in controlled low limits, thus protecting biological molecules from oxidative damage [24]. Nickel containing superoxide dismutase (Ni-SOD) has been isolated from several *Streptomyces* species [25]. The enzymatic activity of Ni-SOD [26] however is the same high level as that of Cu, Zn-SOD of about  $10^9 M^{-1}S^{-1}$  per metal center. X-ray crystallographic studies [27, 28] of Ni-SOD revealed a square planar  $N_2S_2Ni^{II}$  in reduced form and a square-pyramidal  $N_3S_2Ni^{III}$  in oxidized form as shown in Scheme 1. The SODs disproportionate the toxic superoxide radical anion ( $O_2^-$ ) to molecular oxygen ( $O_2$ ) and hydrogen peroxide ( $H_2O_2$ ) of their redox active metal centers [29] such as Cu, Ni, Fe, Mn. All the SOD's including Cu, Zn-SOD and Mn-SOD in mammalian systems, Fe-SOD and Ni-SOD in bacterial systems employ the two steps "Ping-Pong" mechanism **which consist of two diffusion-controlled steps**, shown in Equation (1) and (2), where ME is the redox active centre of metalloenzymes capable of both oxidizing and reducing superoxide properties.



In continuation of our previous work **on copper (II) and nickel(II) Schiff base complexes** [30], in this article, we reported the syntheses, spectroscopic characterization and catalytic activity of SOD-like metallic complexes based on imine ligands containing 2-aminothiophenol moiety which can be considered as possible models of functional SOD mimics. The Schiff bases and its metallic complexes have been synthesized and tested and have shown antioxidant SOD-like activity *in vitro*, while the double Schiff base ligands did not exhibit the SOD activity. These complexes were also tested for their *in vitro* antibacterial screening activities against three bacteria (*Streptococcus aureus*, *Salmonella typhi*, and *Escherichia coli*) comparing with the Schiff bases and double Schiff bases. Most of the complexes have higher antibacterial activities than those of the free Schiff bases, double Schiff bases and the control. All the synthesized metal complexes are found to be binuclear and confirmed by elemental analyses, magnetic susceptibility measurements and ESR spectroscopy. Very few Schiff bases with different structure have been synthesized and characterized as disulfide bonds reported so far [31, 32]. The oxidized form of Schiff bases was also characterized by single crystal X-ray analysis. Several attempts were made to develop the single crystal of the complexes but failed due to the insolubility of the complexes in common organic solvents. The SOD activities have been measured using alkaline DMSO as a source of superoxide radical ( $O_2^-$ ) and NBT (nitro blue tetrazolium) as a ( $O_2^-$ ) scavenger.



**Scheme1.** Structure and functional model of Ni-SOD active sites.

## 2. Experimental

### 2.1 Materials used for synthesis

All chemicals were commercially available and were used as received. Reagents used for the physical measurements were of spectroscopic grade and were used without further purification.

### 2.2. Syntheses

#### 2.2.1. Synthesis of (Z)-2-(2-methoxybenzylideneamino) benzenethiol ( $HL^1$ )

A solution of 2-methoxybenzaldehyde (10 mmol, 1.36g), in 20 mL of absolute ethanol at 60°C was slowly added to a solution of 2-aminothiophenol (10 mmol, 1.25g) in 20 mL of absolute ethanol at 60°C and the mixture stirred for 6h at 60°C under the inert atmosphere of argon. After removal of the solvents, the yellow precipitate was obtained and washed with methanol. Then, the product was dried in vacuo at room temperature. The purity was checked by elemental analysis. Isolated yield: 78%. M p.: ~92°C. **Anal. Found for  $C_{14}H_{11}NOS$ ,  $HL^1$  (%)**: C, 69.98; H, 4.59; N, 5.80. **Calcd. (%)**: C, 70.01; H, 4.62; N, 5.81. **FAB- mass (m/z) Anal. : 241.06, Calcd. : 241**

#### 2.2.2 Synthesis of 3-((Z)-(2-mercaptophenylimino) methyl)-benzonitrile ( $HL^2$ )

2-aminothiophenol (10 mmol, 1.25g) and 3-formylbenzonitrile (10 mmol, 1.31g) were mixed and then fused together at 80°C under the inert atmosphere of argon with constant stirring for 10h. The mixture was then cooled, and absolute ethanol (60mL) was added. The mixture was stirred for 15 min and then filtered off. The filtrate volume reduced to about 10mL and resulting in the formation of a green precipitate. The precipitate was decanted off and washed twice with methanol (2×10mL). Then, the product was dried in vacuo at room temperature and stored in a  $CaCl_2$  desiccator. The purity was checked by elemental analysis. Isolated yield: 75%. M p.: ~154°C. **Anal. Found for  $C_{14}H_{10}N_2S$ ,  $HL^2$  (%)**: C, 70.56; H, 4.23; N, 11.76. **Calcd. (%)**: C, 70.53; H, 4.25; N, 11.78. **FAB- mass (m/z) Anal. : 238.31, Calcd. : 238.**

### 2.2.3 Synthesis of 2-((E)-(2-methoxyphenylamino) methyl)-6-bromo-4-nitrophenol (H<sub>2</sub>L)

This ligand was synthesized in the same manner as HL<sup>1</sup> and HL<sup>2</sup>, except that the 3-bromo-2-hydroxy-5-nitrobenzaldehyde (10 mmol, 2.46g) was used in 20 mL of absolute ethanol at 70°C and heated on a water bath at 58°C. The filtrate volume reduced to about 10mL and resulting in the formation of a brown red precipitate. The precipitate was decanted off and washed twice with diethyl ether (2×10mL). Then, the product was dried in vacuo at room temperature and stored in a CaCl<sub>2</sub> desiccator. Its purity was checked by elemental analysis. Isolated yield: 70%. M p.: ~180°C. **Anal. Found for C<sub>13</sub>H<sub>9</sub>BrN<sub>2</sub>O<sub>3</sub>S, H<sub>2</sub>L (%)**: C, 44.21; H, 2.57; N, 7.93. **Calcd. (%)**: C, 44.23; H, 2.58; N, 7.92. **FAB- mass (m/z) Anal. : 353.19, Calcd. : 353.**

### 2.2.4 Synthesis of copper dimer complex [Cu<sub>2</sub>(L<sup>1</sup>)<sub>2</sub>]<sup>2+</sup> 1 and [Cu<sub>2</sub>(L<sup>2</sup>)<sub>2</sub>(H<sub>2</sub>O)<sub>2</sub>] 2

To an ethanolic solution of Cu (OCOCH<sub>3</sub>)<sub>2</sub>.H<sub>2</sub>O (1.0 mmol, 0.199g) was added dropwise to a solution (10mL) of HL<sup>1</sup> (2.0 mmol, 0.592 g) in the presence of triethylamine(3.0mmol, 40μL) as base. The reaction mixture was heated with constant stirring on a water bath at 70°C for 6-8h. The resulting dark green solution was evaporated and the green precipitate products were recovered from mother liquor which were filtered, washed with methanol and stored in a desiccator over CaCl<sub>2</sub>. Complex 2 was synthesized in the same manner as complex 1, except that the HL<sup>2</sup> (2.0 mmol, 0.476 g) in the presence of triethylamine(3.0mmol, 40μL) as base. Their purity was checked by elemental analysis. Isolated yield (65-68%). **Anal. Found for C<sub>28</sub>H<sub>24</sub>Cu<sub>2</sub>N<sub>2</sub>O<sub>2</sub>S<sub>2</sub>1 (%)**: C, 54.98; H, 3.95; N, 4.58. **Calcd. (%)**: C, 55.00; H, 3.97; N, 4.60. **FAB- mass (m/z) Anal.:** 611.72, **Calcd.:** 612. **Anal. Found for C<sub>28</sub>H<sub>22</sub> Cu<sub>2</sub> N<sub>4</sub>O<sub>2</sub> S<sub>2</sub> 2(%)**: C, 52.73; H, 3.48; N, 8.79. **Calcd. (%)**: C, 52.76; H, 3.51; N, 8.82. **FAB- mass (m/z) Anal. : 636, Calcd. : 638.**

### 2.2.5 Synthesis of nickel dimer complex [Ni<sub>2</sub>(L)<sub>2</sub>] 3

The H<sub>2</sub>L (2.0 mmol, 0.592 g) dissolved in ethanol (20 mL) in the presence of triethylamine(3.0mmol, 40μL) and was reacted with Ni (OAc)<sub>2</sub>.4H<sub>2</sub>O (1.0 mmol, 0.249 g) in constant stirring and reflux(80°C). The dark red solution was stirred during 5h. The resulting red solution was evaporated and the dark red precipitate product were recovered from mother liquor which were filtered, washed with methanol and stored in a desiccator over CaCl<sub>2</sub>. This complex gives satisfactory elemental analysis. Isolated yield (60%). **Anal. Found for C<sub>26</sub> H<sub>14</sub> Br<sub>2</sub> N<sub>4</sub> Ni<sub>2</sub> O<sub>6</sub>S<sub>2</sub> 3 (%)**: C, 38.09; H, 1.72; N, 6.83 **Calcd. (%)**: C, 38.11; H, 1.73; N, 6.82. **FAB- mass (m/z) Anal. : 819.74, Calcd. : 819.**

### 2.3. Physical measurement

Elemental analyses (CHN) were performed on an Elementar Vario EL III Carlo Erba 1108 analyzer. FAB mass spectra were recorded on a JEOL SX 102/DA 6000 mass spectrometer using xenon (6kV, 10mA) as the FAB gas. The accelerating voltage was 10 kV and the spectra were recorded at room temperature (RT) with

m-nitro benzoyl alcohol as the matrix. Magnetic susceptibility measurements of powder samples of complexes were made on a Gouy balance using a mercury (II) tetrathiocynato cobaltate (II) as calibrating agent ( $\chi_g=16.44\times 10^{-6}$  c.g.s. units). All the experimental data were corrected for diamagnetic were estimated from Pascal table and temperature independent paramagnetism (TIP). The molar ion exchange was measured using a systronics digital conductivity meter (TDS-308) using a  $10^{-3}$ M solution in DMSO. UV-Vis spectra were recorded at 25°C on a Thermo scientific UV-Vis recording spectrophotometer Evolution-3000 in quartz cells. Fluorescence spectra were recorded at room temperature on a Horiba Scientific Fluoromax-4 spectrofluorometric in quartz cell. IR spectra were recorded in KBr medium on a Shimadzu IR Affinity -1S Fourier transform infrared spectrophotometer X-band (~9.4 GHz). The ESR spectra were recorded with a Varian E-line Century Series. ESR Spectrometer equipped with a dual cavity and operating at X-band of the 100 kHz modulation frequency at room temperature. Tetracyanoethylene (TCNE) was used as field marker ( $g=2.00277$ ). The solution was deoxygenated by purging nitrogen gas.

#### **2.4. Scavenger measurements of superoxide radicals**

The SOD- like activities of all the complexes was investigated by NBT-DMSO assay. The in vitro SOD activity was measured using alkaline DMSO as a source of superoxide radical ( $O_2^-$ ) and nitroblue tetrazolium chloride (NBT) as ( $O_2^-$ ) scavenger [33]. In general, 400 $\mu$ l sample to be assayed was added to a solution containing 2.1 ml of 0.2 M potassium phosphate buffer (pH 8.6) and 1ml of 56  $\mu$ M of alkaline DMSO solution was added while string. The absorbance was then monitored at 540 nm against a sample prepared under similar condition except NaOH was absent in DMSO. A unit of superoxide dismutase (SOD) activity is concentration of complex, which causes 50% inhibition of alkaline DMSO mediated reduction of nitrobluetetrazolium chloride (NBT).

#### **2.5. Antibacterial activity**

The in *vitro* biological activity of the investigated Schiff base ligands and their metal complexes **1-3** were tested against three bacteria *Streptococcus aureus*, *Salmonella typhi* and *Escherichia coli* by the paper disc diffusion method [34] using nutrient agar as the medium and chloramphenicol as the control. DMSO solvent was used as positive control. Each of the complexes was dissolved in DMSO and the solutions of different concentrations (10-30mM) were prepared separately. The liquid medium containing the bacterial subcultures was autoclaved for 20 min at 121°C and at 15 lb pressure before inoculation. The bacteria were then cultured for 24h at 36°C in an incubator. Nutrient agar was poured into a plate and allowed to solidify. The test compounds (DMSO solutions) were added drop wise to a 10 mm diameter filter paper disc placed at the center of each agar plate. The plates were then kept at 5°C for 1 h then transferred to an incubator maintained

at 36°C. The width of the growth inhibition zone around the disc was measured after 24 h incubation. All the experiments were performed in triplicates.

## 2.6. Crystal structure determination

To unambiguously confirm the structure of double Schiff bases, an X-ray is desired. Single crystal X-ray diffraction data for double Schiff base ligands were collected at 293(2) and 296(2) K. The X-ray diffraction measurements of double Schiff bases were collected on CCD detector based diffractometer (SMART, APEX-II) from Bruker-Nonius CAD-4/MACH3, AX<sub>s</sub> and CrysAlisPro, Oxford diffractometer using graphite monochromatized Mo-K $\alpha$  radiation ( $\lambda=0.71073\text{\AA}$ ) for the double Schiff bases from a fine focus sealed tube radiation source. The crystal orientation, cell refinement and intensity measurements were made using the program CAD-4PC performing  $\psi$ -scan measurements. Multi-scan absorption corrections were applied empirically to the intensity values ( $T_{\max}=0.7455$  and  $T_{\min}=0.6844$  for  $\mathbf{L}^1_{\mathbf{a}}$ ,  $T_{\max}=0.5615$  and  $T_{\min}=0.4411$  for  $\mathbf{L}^2_{\mathbf{a}}$  and  $T_{\max}=0.9295$  and  $T_{\min}=0.9185$  for  $\mathbf{H}_2\mathbf{L}_{\mathbf{a}}$ ) using the program SADABS [35] or SCALE3 ABSPACK algorithm within CRYALISPRO. The crystal structures were solved by the direct or charge-flipping methods using programs SHELXT, SIR 2014[36], OLEX2 solve [37] or SUPERFLIP [38] and refined by the full-matrix least square procedure with SHELXL or CRYSTALS. Geometrical analysis was performed using SHELXL on F2 or CRYSTALS. All non-hydrogen atoms were refined anisotropically. All the hydrogen atoms were geometrically fixed and allowed to refine using isotropic thermal parameters. The crystallographic data of double Schiff base ligands have been deposited with the Cambridge Crystallographic Data Centre as supplementary publication CCDC Nos. 1536404, 1573259 and 1561750 for  $\mathbf{L}^1_{\mathbf{b}}$ ,  $\mathbf{L}^2_{\mathbf{a}}$  and  $\mathbf{H}_2\mathbf{L}_{\mathbf{a}}$ , respectively.

## 3. Results and discussion

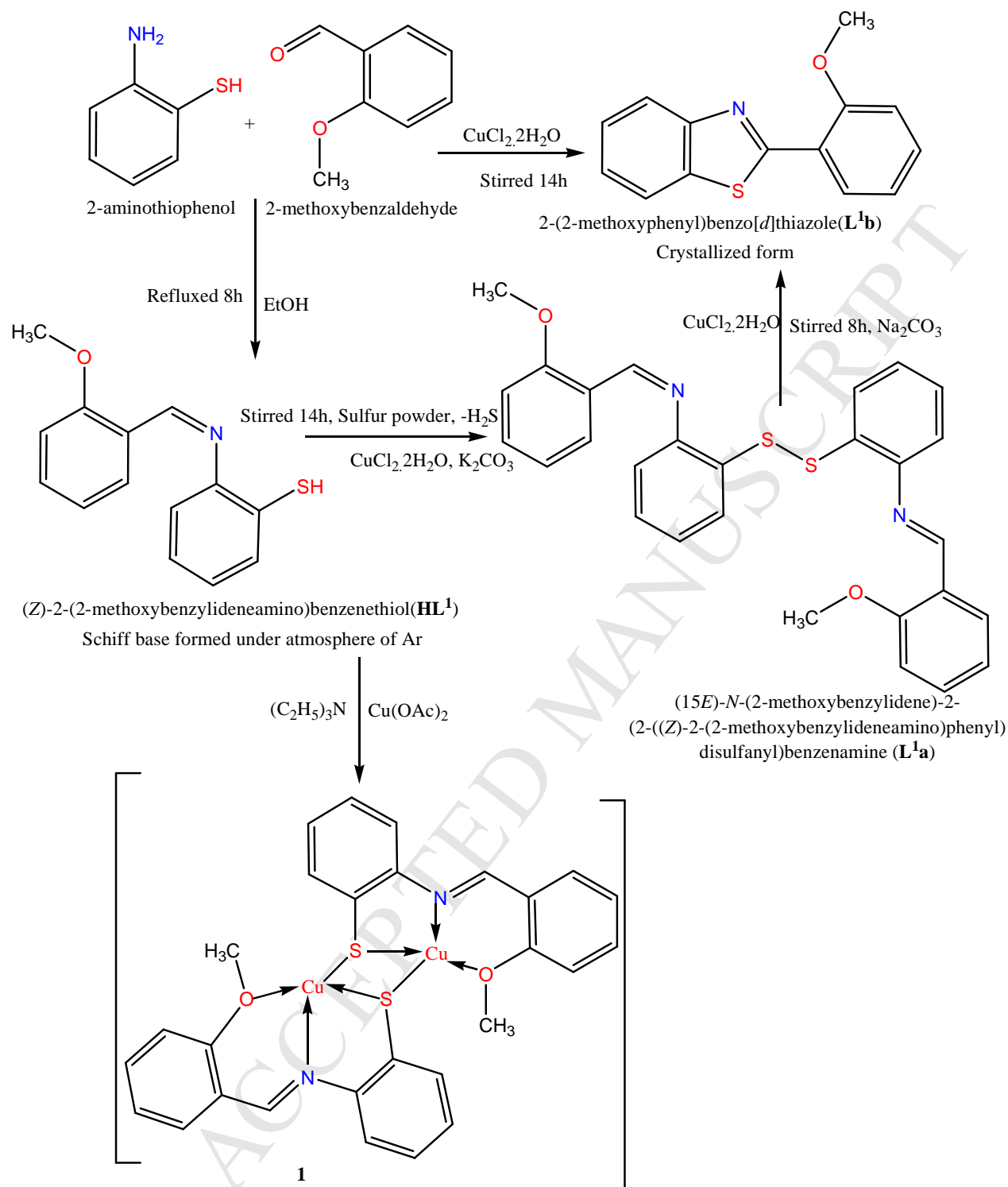
### 3.1 Synthesis and characterization

The composition and molecular formulas of the three dimer complexes with ONS/SNN or N, S donor Schiff base ligands were determined by elemental analyses. The protocol used for the syntheses for tridentate Schiff bases, double Schiff base ligands and their dimer complexes **1-3** was given in Scheme 2-4. The most plausible geometry for the 1:2 complexes appeared to be distorted square-planar or tetrahedral environments. The isolated products were characterized by various physicochemical and spectroscopic techniques. These complexes are non-electrolyte in nature. In **these metallic** complexes, Schiff base ligands acted as a chelating agent towards the metal ions as a tridentate ligands via azomethine-N atoms, one oxygen/ nitrogen atoms and CuCu and NiNi metal centers were bridged by the S atoms and thus facilitated the linkage of two units (Scheme 2-4). Similar dimer copper (II) and nickel (II) complexes were reported by some other workers [39]. Furthermore, the SH groups of two Schiff bases ( $\mathbf{HL}^1/\mathbf{HL}^2/\mathbf{H}_2\mathbf{L}$ ), were oxidized to form double Schiff

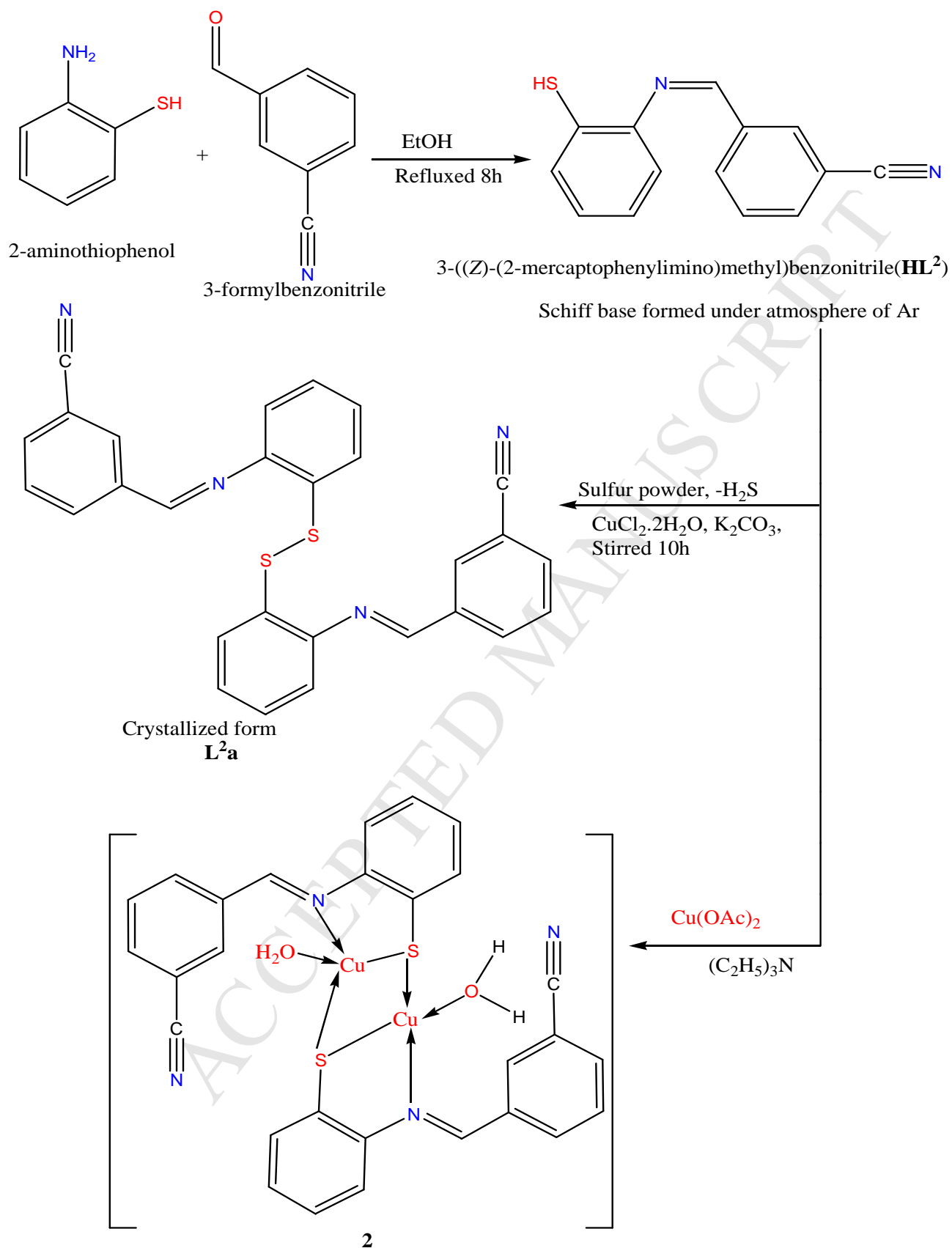
bases during the formation of crystalline form in the air [40-42]. The suitable single crystals of double Schiff base ligands were obtained by slow diffusion of diethyl ether into a concentrated solution of Schiff bases in DMF in the presence of  $\text{CuCl}_2 \cdot 2\text{H}_2\text{O}$  and bases ( $\text{K}_2\text{CO}_3$ ,  $\text{K}_3\text{PO}_4$ ,  $\text{Na}_2\text{CO}_3$  and  $\text{NaOH}$ ) after five days at room temperature and its structure were determined by X-ray crystallography, whereas suitable single crystals could not be grown for the metal complexes by different methods. Although, a lot of Schiff bases with different structures have been synthesized and characterized, however, little attention has been given to the Schiff bases which include disulfide bonds. We are also surprising to get this new disulfide Schiff bases which are unique and there are some literature on this kind of crystal structure having disulfide bonds [40-42]. **As shown in Scheme 2-4, a tentative reaction pathway for the formation of dimeric complexes 1-3 was proposed.** The complexes are isolated as binuclear and confirmed by elemental analyses, magnetic susceptibility measurements, IR and ESR spectroscopy.

### ***3.2 Molar conductivity and elemental analysis***

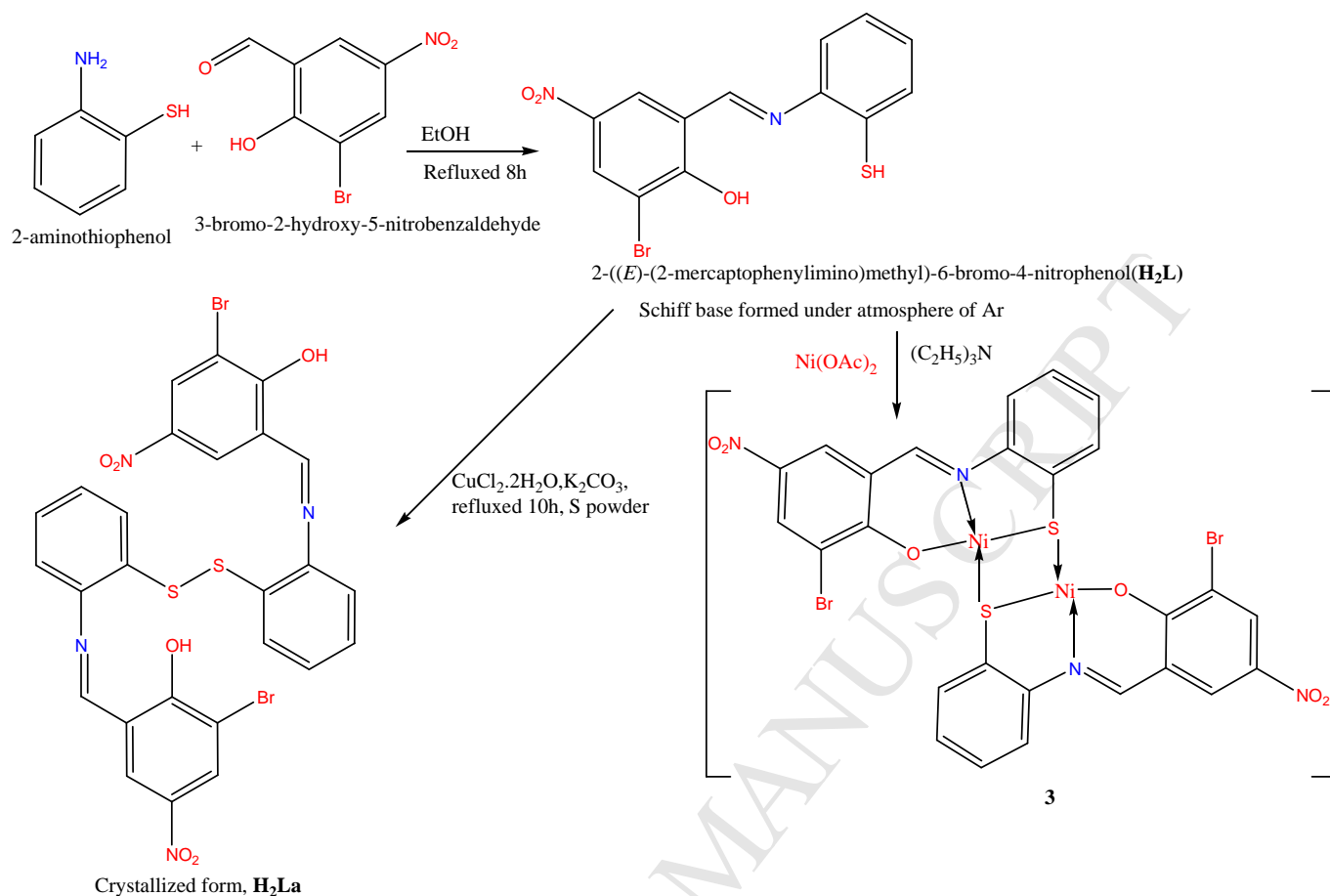
The molar conductivity of the complexes ( $1 \times 10^{-4}$  M) was measured in DMSO solution at room temperature. The molar conductivity values of all complexes were in the range of  $1.58\text{-}5.83 \Omega^{-1}\text{cm}^2\text{mol}^{-1}$ , indicating the non-electrolyte nature of these **metallic** complexes [43]. The elemental analyses of the complexes indicated that the absence of counter ions in the formula. The obtained elemental analyses results were in good agreement with those calculated for the suggested formula of Schiff base ligands and metal complexes. In complexes **1-3**, it has been observed that Schiff base ligands either behaves as tridentate (ONS/SNN) and/ or bidentate-N, S donor ligands in the 1:2 complexes.



**Scheme 2.** The proposed reaction pathway of the **HL<sup>1</sup>**, **L<sup>1a</sup>**, **L<sup>1b</sup>** ligand and dimer copper complex **1**.



**Scheme 3.** Proposed reaction pathway of the **HL<sup>2</sup>**, **L<sup>2a</sup>** ligand and dimer copper complex **2**.



**Scheme 4.** Proposed reaction pathway of the **H<sub>2</sub>L**, **H<sub>2</sub>La** ligand and dimer nickel complex **3**.

### 3.3 Description of the molecular structures of double Schiff base ligands

The suitable single crystals of double Schiff base ligands were obtained by slow diffusion of diethyl ether into a concentrated solution of Schiff bases in DMF in the presence of bases including K<sub>2</sub>CO<sub>3</sub>, K<sub>3</sub>PO<sub>4</sub>, Na<sub>2</sub>CO<sub>3</sub> and NaOH and its structure were determined by X-ray crystallography, whereas suitable single crystals could not be grown for the metal complexes by different methods. The ORTEP structures of double Schiff bases are shown in Figs.1-3, respectively. Crystallographic data and molecular structure refinement important inter atomic parameters are given in Table 1. Selected bond angles and lengths for double Schiff base ligands were given in Table2. The 2-(2-methoxyphenyl) benzo[*d*]thiazole ligand (**L<sup>1</sup><sub>b</sub>**) was crystallized in the centro-symmetric monoclinic system of the space group P2<sub>1</sub>/*n*,  $a=7.3276(6)\text{Å}$ ,  $b=12.6798(11)\text{Å}$ ,  $c=12.7253(11)\text{Å}$ ,  $\alpha=90^\circ$ ,  $\beta=96.484(2)$ ,  $\gamma=90^\circ$  and  $Z=4$ . Here, the Schiff base, 2-(2-methoxyphenyl) benzo[*d*]thiazole (**L<sup>1</sup><sub>b</sub>**) act as the bidentate N, S-donor ligand (Scheme2). It is an aromatic heterocyclic compound with the chemical formula C<sub>14</sub>H<sub>11</sub>NOS [44]. It consists of a five-membered 1, 3-thiazole ring fused to a benzene ring. Its derivatives are used in inorganic chemistry for building polydentate ligands [1]. Furthermore, The 2-(2-methoxyphenyl) benzo[*d*]thiazole ligand are bicyclic ring system and constitute an

important class of compounds with profound interest to medicinal/ industrial chemists as compounds bearing the benzothiazolyl moiety[45]. To the best of our knowledge, the application of 2-aminothiophenol for the synthesis of 2-(2-methoxyphenyl) benzo[*d*]thiazole ligand and its single crystal X-ray determination crystal is still rare [45].

The  $\text{HL}_a^2$  was crystallized in the monoclinic system of the space group  $C/2c$ ,  $a=14.8849(18)$  Å,  $b=8.3000(9)$  Å,  $c=19.664(2)$  Å,  $\alpha=90^\circ$ ,  $\beta=100.625(9)$ ,  $\gamma=90^\circ$  and  $Z=4$ . The double Schiff base  $\text{H}_2\text{L}_a$  was crystallized in the monoclinic system of the space group  $P-1$ ,  $a=8.2685(12)$  Å,  $b=11.7305(16)$  Å,  $c=14.4154(18)$  Å,  $\alpha=102.618(7)$ ,  $\beta=96.008(7)$ ,  $\gamma=100.367(7)$  and  $Z=2$ . According to the crystal structures (Fig. 2 and 3), these double Schiff bases were contained disulphide bond. Intramolecular S-S bond in the Schiff base ligand was observed in crystalline structure obtained by X-ray crystallography and also its data was obtained by different spectroscopy methods. We are surprising to get this new double Schiff base structures which is unique and there are some literature on this kind of crystal structures of disulfide Schiff bases [46]. The structural parameters which have shown in Table1 are in good agreement with other reported similar compounds [46]. The packing diagram of double Schiff base ligands were shown in Figs.4-6 along a-axis, respectively and this shows that how the disulfide structure arranged donor sites. Furthermore, the SH groups of two tridentate Schiff bases were oxidized to form double Schiff bases as a new class of inorganic compounds with sulfur atoms (Scheme2-4).

### 3.4 IR spectral investigations

The **Schiff base** ligands were characterized by single crystal X-ray analysis, FT-IR spectroscopy and elemental analysis. In order to characterize the binding mode of the Schiff base ligands to the metal ion in the complexes, the IR spectrum of the free ligands was compared with the spectra of the metal complexes. Analysis by FT-IR results in the transmittance spectra in the infrared region ( $400\text{-}4000\text{cm}^{-1}$ ) and register bands or signals (Table 3). The IR spectrum of Schiff base ligands exhibits strong bands at  $1581\text{-}1627\text{cm}^{-1}$ , which can be attributed to  $\nu(\text{C}=\text{N})$  stretching vibration. The IR spectrum for the ligands confirmed the presence of imine and the absence of carbonyl and amine functional groups of the starting materials. Furthermore, the IR spectra data confirms the coordination of Schiff bases through azomethine-N to the metal atoms by shifting the  $\nu(\text{C}=\text{N})$  stretching frequency of free Schiff base ligands to the higher frequency in the range of  $1624\text{-}1632\text{cm}^{-1}$  in complexes. This shift to higher wavenumber may be attributed to the increase in bond order of the carbon to the nitrogen link [47]. The participation of phenolic group is deduced by clarifying the effect of chelation on the  $\nu(\text{C}-\text{O})$  stretching vibration. The shift in  $\nu(\text{C}-\text{O})$  of the phenolic groups from  $1512\text{-}1427\text{cm}^{-1}$  in the free ligands to lower frequencies in the region of  $1311\text{-}1122\text{cm}^{-1}$  for

complexes was observed, indicating the participation of the oxygen atom of phenolic group in coordination to the metal ions[48].

Furthermore, the spectra of Schiff base ligands showed broad bands in  $3051\text{-}2994\text{cm}^{-1}$ , attributed to the stretching vibration of the O-H groups. The absence of the vibration peaks of OH in all complexes exhibits that the OH groups is deprotonated and coordinated[49,50]. The weak bands in the regions of  $509\text{-}543\text{cm}^{-1}$ , and  $540\text{-}430\text{cm}^{-1}$ , in the complexes may be assigned to the  $\nu(\text{M-O})$  and  $\nu(\text{M-N})$ , respectively[51]. Again,  $\nu(\text{C-S})$  in complexes shifted to higher frequencies from  $721$  to  $740\text{-}790\text{cm}^{-1}$ , which is evidence of the M-S bond [52]. The bands in  $1114\text{-}1465\text{cm}^{-1}$  regions are due to the skeletal stretching vibration of C=C backbone in the benzene rings. Several weak bands observed in the region  $3000\text{-}2700\text{cm}^{-1}$  is most likely due to the aromatic C-H groups. Also, in these compounds the common bands at  $750\text{-}753\text{cm}^{-1}$  were assigned to the C-S and S-S stretches [53]. The vibrational peak of  $\text{NO}_2$  in the IR spectrum of  $\text{H}_2\text{L}$  is observed in  $1597$  and  $1573\text{cm}^{-1}$ . The IR spectra of Schiff base ligands and **its dimeric complexes** were shown in Figs. 7-11. The IR data of ligand showed that the Schiff bases was coordinated to the metal ions in a tridentate-ONS/ NNS or bidentate-NS manner. The infrared spectra of ligands and their complexes were agreed with the proposed molecular structures.

### 3.5 FAB-mass study

The FAB- mass (m/z) spectra suggested that the present binuclear complexes **1-3** showed dimeric nature. The Schiff base ligands and their copper (II) and nickel (II) complexes, provide strong evidence for the formation of these compounds and exhibits peaks at higher molecular weights. Thus, mass spectra of tridentate Schiff base ligands ( $\text{HL}^1/\text{HL}^2/\text{H}_2\text{L}$ ), double Schiff base ligands ( $\text{L}_a^1/\text{L}_a^2/\text{H}_2\text{L}_a$ ) and **complexes 1-3** showed the highest mass peaks at obs. (calcd.):  $241(241)$ ,  $238(238)$ ,  $353(354)$ ,  $485(486)$ ,  $474(475)$ ,  $701(704)$ ,  $611(612)$ ,  $636(638)$  and  $819(820)$ , respectively. **Some representative FAB-mass (m/z) spectra of metallic complexes are presented in Figs. 12-14, respectively.**

### 3.6 Electronic spectra, fluorescence features and magnetic moment studies

The magnetic susceptibility measurements for binuclear complexes **1-3** were measured in the solid state. The observed magnetic moments of these complexes are quite close to the value expected for the other copper (II) and nickel (II) complexes. The value of magnetic moment at room temperature allows to suppose that the complex **1** and **2** are built up by the antiferromagnetic coupled binuclear cluster ( $S=1$  state) and that the magnetism of complex **3** are due to the unpaired one-spin system ( $S=1/2$ ), with mild intermolecular interactions. Complex **1** and **2** are paramagnetic in solid state at room temperature as expected from  $d^9$  electronic configuration of Cu (II) ion. The binuclear complex **1** and **2** has substantially reduced magnetic moments  $1.51\text{ BM}$ . for **1** and  $1.48\text{ B.M.}$  for **2**, consistent with proposed dimeric structures, suggesting the

possibility of spin-coupled system [54]. This behavior is ascribed to a paramagnetic species containing two antiferromagnetic ally coupled Cu (II) ions. The antiferromagnetic behavior occurs when two copper (II) coordination spheres connect at axial sites of two square planar units. As expected, room temperature magnetic moments values of complexes **3** differ markedly from that of the complex **1** and **2**. The observed magnetic moment value of complex **3** was 3.61 B.M., in agreement with an unpaired one spin ( $S = \frac{1}{2}$ ) system.

The UV-Vis spectral data of tridentate Schiff base ligands and its complexes **1-3** were recorded (**Fig.15**). The electronic absorption spectrum provides reliable information about the ligand arrangement in transition metal complexes. The electronic spectra of free tridentate ligands exhibits absorption bands at 430-450 and 370-390nm, which are assigned to the  $n-\pi^*$  transitions of the imine moiety and  $\pi-\pi^*$  transitions of phenyl rings, respectively. The electronic spectrum of **1** of HL<sup>1</sup> exhibited three bands, 450, 380 and 268nm, which may be assigned to d-d,  $n-\pi^*$  and  $\pi-\pi^*$  transitions, respectively. The electronic spectra of **2** shows a broad band at 440nm due to d-d transition and at 367nm which may be due to  $n-\pi^*$  band of the imine. Complex **2** of HL<sup>1</sup> has another band centered at 272nm which is assigned to  $\pi-\pi^*$  transitions of phenyl rings [55, 56]. Complex **3** of H<sub>2</sub>L shows bands at 450, 380 and 280 nm which may be assigned to d-d,  $n-\pi^*$ , and  $\pi-\pi^*$  transitions, respectively. All these observations make us to suggest the structure of these complexes.

Fluorescent properties (absorption and emission properties) of tridentate Schiff base ligands and its complexes were investigated at room temperature in DMSO (**Fig. 16**). The tridentate Schiff base ligands has two absorption maxima; the first one is between 260-275nm and the second one is between 350-385nm. For the first absorption maxima appeared in the same region, the second absorption maxima shifted to lower wavelengths between 410-420nm, presumably due to the complete transfer of the electrons from the ligands to the metal ion. The extinction coefficients at the shorter absorption maxima are higher than the extinction coefficients at the longer absorption maxima for ligands and all the complexes. Complexes have one emission band, which is between 410-480nm. The fluorescence quantum efficiencies of the ligands and the complexes with a standard of quinine sulfate indicated that the highest quantum yield values were obtained for all the tridentate Schiff base ligands compared to its complexes [57].

### 3.7 ESR study

ESR is an ideal, complementary technique to study materials with unpaired electrons. Best evidence for the proposed structures of the binuclear complexes comes from the magnetic measurements and ESR spectra. ESR spectra of binuclear complex **1** and **2** were recorded in polycrystalline state and also in 100%DMSO and at liquid nitrogen temperature (77K). The ESR spectra of **1** and **2** are shown in **Figs.17 and 18**. Basic spectral characteristics at both temperatures are the same with slightly better resolution at LNT. Conforming the magnetic measurements, the polycrystalline ESR spectra of both complexes showed the spectral features of

an antiferromagnetically coupled binuclear species: (i) The  $\Delta Ms = \pm$  'half filled' signals is observed at 1700G, (ii)  $\Delta Ms = \pm 1$  region shows two broad signals at -2960G and 3200 G, -3080G and 3400 G, respectively, and is characteristics of isotropic spectral feature. Interestingly, the EPR spectra of **1** and **2** are similar. For each complex spectral feature of RT and LNT was also similar. The  $g = 2$  signals for these complexes was broad and nearly isotropic. This is suggestive of the spin-spin interactions arising due to solid effect [58]. The room temperature polycrystalline ESR spectra of **1** and **2** exhibits the usual shape line for mononuclear copper (II) complexes with  $g_{\parallel} > g_{\perp} > 2.0023$ , indicating axial symmetry ( $d_{x^2-y^2}$ ).

Both complexes exhibits two  $g_{\text{eff}}$  ( $g_{\parallel} = 2.058 \pm 0.003$ ,  $g_{\perp} = 2.268 \pm 0.001$  with  $g_{\text{av}} = 1.68002 \pm 1$  for **1** and  $g_{\parallel} = 2.246 \pm 0.001$ ,  $g_{\perp} = 2.268 \pm 0.001$  with  $g_{\text{av}} = 1.5862 \pm 1$  for **2**). It should be pointed out that these values are quite close to that of Cu, Zn-SOD ( $g_{\parallel} = 2.271$ ,  $g_{\perp} = 2.083$ ) [59]. The value of  $g_{\text{eff}}$  and the shape of the ESR signals of the copper (II) complexes suggest square planar coordination around the Cu (II) ions [60]. The positive contribution of the  $g_{\text{eff}}$  values over the free electron value (2.0023) indicates an increase in the covalency between the ligands and the Cu (II) ions in the complexes. The magnetic moment for **1** and **2** are  $\mu_{\text{eff}} = 1.51$  and 1.48, respectively at room temperature. The calculated  $\mu_{\text{eff}}$  values of the magnetic moments may be due to the antiferromagnetic interaction between the two electrons in the two adjacent Cu (II) ions. Since the  $g_{\parallel}$  and  $g_{\perp}$  values are closer to 2 and  $g_{\parallel} > g_{\perp}$ , a tetragonal distortion around the Cu (II) ion is suggested. The trend ( $g_{\parallel} > g_{\perp} > g_e(2.0023)$ ) shows that the unpaired electron is localized in the  $d_{x^2-y^2}$  orbital in the ground state of Cu(II) and spectra were characteristics of axial symmetry environments ( $g_{\parallel} > g_{\perp} > 2.0023$ ), with an electronic configuration  $3d^9$ , electron spin  $S=1/2$  and nuclear spin  $I=3/2$ . The value of  $g_{\parallel} > 2.3$  is characteristics of an ionic environment and  $g_{\parallel} < 2.3$  indicates a covalent environment in metal-ligand bonding. As observed in the investigated spectra, complex **3** show  $g_{\parallel}$  value  $< 2.3$ , which is a feature observed in copper (II) complexes with covalent bonds [61,62]. The hyperfine coupling constant for **1** and **2** was 170G and 172G, respectively.

The exchange coupling interaction between two Cu (II) ions is explained by the Hathaway expression [63].

$$G = (g_{\parallel} - 2.0023) / (g_{\perp} - 2.0023) \quad (4)$$

According to Hathaway, if the value  $G$  is greater than 4 ( $G > 4.0$ ), the exchange interaction is negligible whereas when the value of  $G$  is less than 4 ( $G < 4.0$ ), a considerable exchange coupling is present in a solid complex. As observed in the spectra of complexes **1-3**,  $G$  value was less than 4 (3.37 for **1** and 3.65 for **2**), indicating considerable exchange interaction in this complex.

### 3.8 SOD-like activity

The SOD-like activities of tridentate Schiff base ligands and its complexes **1-3** were investigated by NBT-DMSO assay, and the catalytic activity towards the dismutation of superoxide ion was measured. The  $IC_{50}$  value is considered the concentration equivalent to one unit of SOD activity. The coordination arm with two

tridentate Schiff base ligands provide a stable and flexible environment to that in the active sites of the native enzymes, insuring the stable existence of the native enzyme and the stable existence of the complexes. In this work, the SOD-like activities for the three binuclear complexes were measured. These complexes exhibit effective catalytic activity towards the dismutation of superoxide anions. The average suppression ratio against  $O_2^-$  increases with increasing concentration in the range of the tested compounds. The SOD activity data showed that complexes **1-3** exhibited effective SOD activity, which is indicative of their potential application as an antioxidant. The  $IC_{50}$  values presented by complexes were compared with earlier reported values for nickel (II) and copper (II) Schiff base complexes and Cu, Zn-SODs (determined by different research groups) [64-70]. The catalytic activity of Ni-SOD [25], however, is a same high level as that of Cu, Zn-SOD at about  $10^9(ML^{-1})^{-1}S^{-1}$  per metal center [26]. The representative graph showing  $IC_{50}$  data of the SOD activity of tridentate Schiff base ligands and compounds are presented in **Figs.19 and 20**. The results (Table 4) indicated that the prepared compound is more efficient antioxidant than vitamin C, which is the standard superoxide dismutase [69].

Interestingly, the double Schiff base ligands did not exhibit the SOD activity. Complex **1** exhibits more active scavenging effects against  $O_2^-$  than  $HL^1$  and complex **2** of  $HL^2$  and complex **3** of  $H_2L$  under the same conditions. The scavenging effect of the complexes may be ascribed to the chelating function of Schiff base with metal ions to achieve significant activity of radical scavenging activity [70]. Schiff base complex **1-3** show lower  $IC_{50}$ , and exhibits higher SOD activity. The  $IC_{50}$  values for tridentate Schiff base ligands and its complexes **1-3** are 62, 59, 56, 44, 41, and 39  $\mu mol dm^{-3}$ , respectively. The activities of these complexes are similar to those of the other complexes [71, 72]. They are among the most active model compounds but are somewhat less active than the native enzyme ( $IC_{50}=0.04\mu mol dm^{-3}$ ). The kinetic catalytic constant for complexes **1-3** were  $3.75\times 10^4$ ,  $5.52\times 10^4$  and  $4.12\times 10^4(ML^{-1})^{-1}s^{-1}$ , respectively. Values of the catalytic rate constant for superoxide disproportionation clearly showed that these complexes can be used as superoxide scavengers. The  $IC_{50}$  data of SOD assay along with kinetic catalytic constants of compounds  $k_{MCCF} = k_{NBT} [NBT] / IC_{50}$ , where  $k_{NBT} (pH=7.8) = 5.94\times 10^4 M^{-1}S^{-1}$  [73, 74] are listed in Table 4. Comparison of  $k_{MCCF}$  of metal complexes revealed that the geometry around M (II) contributes to modulate SOD activity, with **1** to being best suited to react with superoxide radical. On the basis of above results and early suggested catalytic mechanism [75], a possible mechanism for catalytic process is proposed as follows: First a superoxide anion ( $O_2^-$ ) is attracted and bounded by M (II) ion with all coordination sites. Second, a superoxide anion ( $O_2^-$ ) gives up its electron and form an oxygen molecule, and then the electrically neutral oxygen molecule leaves. Third, another superoxide anion ( $O_2^-$ ) is attracted and bounded by M (I) ion. Fourth, the superoxide anion

(O<sub>2</sub><sup>-</sup>) will accept an electron from M (I) ion and two protons from the buffer solution, and then form a H<sub>2</sub>O<sub>2</sub> molecule. Finally, electrically neutral hydrogen peroxide leaves, completing a catalytic cycle.

### 3.9 Biological screening activity

Antibacterial activities were estimated by MIC (mm) as shown elsewhere [76]. The present complexes were tested for their *in vitro* antibacterial activities against three bacteria against three bacteria *Streptococcus aureus*, *Salmonella typhi* and *Escherichia coli* comparing with tridentate Schiff base ligands. The results (Table 5) of antibacterial activities of dimeric complexes of together with the results of the Schiff bases and of the double Schiff bases as comparison are shown in **Figs.21 and 22**. The Schiff bases shown a wide spectrum of antibacterial activities against the test organisms and especially, show effective activities against *E.coli*. The double Schiff base ligands show modest activities against selected bacterial (*Streptococcus aureus*, *Salmonella typhi* and *Escherichia coli*). The free ligand HL<sup>1</sup>a, which contain bicyclic ring system with N, S donor atoms did not exhibit the growth of test organism. The ligand L<sup>1</sup>b did not show effective antibacterial activities against selected test organisms although the ligand contained no O atoms (bidentate N and S). Any chemotherapeutic agents reduce the growth of microbes by microbial or microstatic mechanism. The tested compounds **1-3** show good antibacterial activity against microorganisms. On comparing the antibacterial activities of free Schiff base ligands, double Schiff base ligands and metal complexes. With these of standard bactericide, it was shown that metal complexes had moderate activity as compared to standard Chloramphenicol but all the complexes were more active than tridentate Schiff base ligands and double Schiff base ligands. These complexes show better activity than the known antibiotic with **1** being more active than **2** and **3**. Complexes **1** and **2** have shown excellent antibacterial activity than *E.coli* comparable to that to *Streptococcus aureus* and *Salmonella typhi*. They inhibit the bacterial growth up to 15-25% µgml<sup>-1</sup> whereas other has poor antibacterial activity [77]. The higher inhibition zone of the metal complexes than those of free tridentate Schiff bases and double Schiff bases can be explaining based on the Overtone's concept and the Chelation theory[78,79]. According to Overtone's concept of cell permeability, the lipid membrane that surrounds the cell favours the passage of only lipid-soluble materials due to which liposolubility is an important factor which controls the antibacterial activity. On chelation, the polarity of the metal ion will be reduced to a greater extent due to the overlap of the ligand orbital and partial sharing of the positive charge of the metal ion with donor groups. Further, it increases the delocalization of π-electrons over the whole chelating ring and enhances the lipophilicity of the complexes. This increased lipophilicity enhances the penetration of the complexes into lipid membranes and blocking of the metal binding sites in the enzymes of microorganisms. These complexes also disturb the respiration process of the cell and thus block the synthesis of proteins which restricts further growth of the microorganism [80, 81].

## Conclusion

In this paper, we reported syntheses, characterization and **catalytic activity of SOD-like metallic complexes of copper (II) and nickel (II) with three** new Schiff base ligands containing 2-aminthiophenol moiety. Elemental analyses showed that all metals reacted with the ligands in a 1:2 molar ratio. The FAB- mass (m/z) spectra suggested that the present binuclear complexes **1-3** showed dimeric nature. The room temperature polycrystalline ESR spectra of **1** and **2** exhibits the usual shape line for mononuclear copper (II) complexes with  $g_{\parallel} > g_{\perp} > 2.0023$ , indicating axial symmetry ( $d_{x^2-y^2}$ ). The X-ray structures of the Schiff base ligands showed that in the crystalline form the SH groups were oxidized to produce a disulfide Schiff bases as a new double Schiff base ligands ( $L^1/L^2/H_2L_a$ ). The Schiff bases shown a wide spectrum of antibacterial activities against the test organisms and especially, show effective activities against *E.coli*. The double Schiff base ligands show modest activities against selected bacterial (*Streptococcus aureus*, *Salmonella typhi* and *Escherichia coli*). Most of the complexes have higher antibacterial activities than those of the free Schiff bases and the control. These complexes show lower biological activity than the known antibiotic chloramphenicol with complex **1** being more active than complex **2** and **3**. Complex **1** exhibits more active scavenging effects against  $O_2^-$  than  $HL^1$  and complex **2** of  $HL^2$  and complex **3** of  $H_2L$  under the same conditions. The double Schiff base ligands did not exhibit the SOD activity

## Acknowledgements

Author thanks the Sophisticated Analytical Instrument Facility (SAIF), Single Crystal X-Ray Division, IIT Chennai and Sophisticated Instrumentation Centre (SIC) IIT Indore for single crystal data collection, respectively. Author wish to thanks to Head RSIC (SAIF), IIT Mumbai for EPR measurements. The Head RSIC (SAIF), Central Drug Research Institute, Lucknow is also thankfully acknowledged for providing analytical and spectral facilities. This work was financially supported from CSIR (Scheme No. 01(2856)/16/EMR-II), New Delhi, India is thankfully acknowledged.

## Supplementary material

CCDC 1536404, 1573259 and 1561750, contain the supplementary crystallographic data for double Schiff base ligands  $L^1/L^2/H_2L_a$ , respectively. Copies of this information can be obtained free of charge via <http://www.ccdc.cam.ac.uk/conts/retrieving.html/> data request/cif, or from The Cambridge Crystallographic Data Centre, 12 Union Road, Cambridge CB2 1EZ, UK, Fax :(+44)-1223-336033/ Email: [deposit@ccdc.cam.ac.uk](mailto:deposit@ccdc.cam.ac.uk).

## References

- [1]. T. Karmakar, Y. Khang, N. Neamati, J. B. Baruah, Polyhedron, 54 (2013) 285.
- [2]. C. Ramalingan, S. Balasubramarian, S. Kabilan, M. Vasudevan, Eur. J. Med. Chem. 39 (2004) 527.

- [3]. M. Karatepe, F. Karatas, *Cell Biochem. Funct.* 24 (2006) 547.
- [4]. D. M.A. El-Aziz, SEH Etaiw, E. A. Ali, *J. Mol. Struct.* 10482013)487.
- [5]. V. Arjunan, S. Sakiladevi, T. Rani, C. V. Mythili, S. Mohan, *Spectrochim. Acta A*, 88 (2012) 220.
- [6]. J. Joseph, G. B. Janaki, *J. Mol. Struct.* 1063 (2014) 160.
- [7].G.Y. Yeap, B. T. Heng, N. Faradiana, R. Zulkifly, M.M. Ito, M. Tannbe, D. Takeuchi, *J. Mol. Struct.* 1012 (2012) 1.
- [8]. S. Arulmurugan, P.H. Kavitha, R. P. Venkatraman, *Rasayan J. Chem.* 3 (2010) 385.
- [9]. C.P. Johnson, J. L. Atwood, J. W. Steed, C.B. Bauer, R. D. Rogers, *Inorg. Chem.* 35(1996) 2602.
- [10]. A. K. Mishra, N. Manav, N. K. Kausik, *Spectrochim. Acta A*, 61 (2005) 3097.
- [11]. N. K. Singh, A. Srivastava, A. Sodhi, P. Ranjan, *Trans. Met. Chem.* 25 (2000) 133.
- [12]. A. Golcu, M. Tumer, H. Dermirelli, R. A. Wheatley, *Inorg. Chim. Acta*, 358 (2005) 1785.
- [13]. R. Ziessel, *Coord. Chem. Rev.* 216 (2001) 195.
- [14]. S. Chandra, S. Gautam, H. K. Rajor, R. Bhatiya, *Spectrochim. Acta A*, 131 (2014) 625.
- [15]. (a). M. M. Tamizh, B. F.T. Cooper, C. L. B. Mcqdonald, R. Karvembu, *Inorg. Chim Acta*, 394 (2013) 391. (b). J. R. Anacona, N. Noriega, J. Camus, *Spectrochim. Acta A*,137 (2015) 16.
- [16]. M. Kalita, T. Bhattacharjee, P. Gogori, P. Barman, R.D. Kalita, B. Sharma, S. Karmakar, *Polyhedron* , 60 (2013) 47. (b). S. Kundu, A. K. Pramanik, A. S. Mondal, T. K. Mondal, *J. Mol. Struct.*1116 (2016)1.
- [17].S. M. Abdullah, G.G. Mohamed, M.A. Zayed, M.S.A. El-EIA, *Spectrochim. Acta Part A*, 73 (2009) 833.
- [18]. M. Ghosh, M. Layek, M. Fleck, R. Saha, D. Bandyopadhyay, *Polyhedron*, 85 (2015) 312.
- [19]. S. Sujarani, A. Ramu, *J. Mol. Struct.* 1079 (2015) 353.
- [20]. **S.Goldstein, G. Czapski, *Free Rad. Res. Comm.* 12(1991) 5.**
- [21].(a).R.N. Patel, A. Singh, K.K. Shukla, D. K. Patel, V. P. Sondhiya, Y. Singh , R. Pandey, *J. Coord. Chem.* 65 (2012) 1381.  
(b). R.N. Patel, A. Singh, K.K. Shukla, D. K. Patel, V. P. Sondhiya, Y. Singh , R. Pandey, *J. Coord. Chem.* 65 (2012)795.
- [22]. R. N. Patel D. K. Patel, V. P. Sondhiya, K. K. Shukla, Y. Singh, A. Kumar, *Inorg. Chim. Acta*, 405(2013)209.
- [23]. J. S. Richardson, K. A. Thomas, B. H. Rubin, D. C. Richardson, *Proc. Natl. Acad. Sci., USA*, 89 (1992) 10405.
- [24]. T. P. Ribeiro, C. Fernandes, K. V. Melo, S. S. Ferreira, J.A. Lessa, R.W. A. Franco, G. Schenk, M. D. Pereira, A. Horn Jr, *Free Radical Biol. Med.*,80 (2015) 67.

- [25]. M.E. Stroup, M. D. Donato, J.A. Tainer, in: A. Messerschmitt, R. Huber, T. Poulos, K. Weighardt (Eds.), *Handbook of Metalloproteins*, Wiley, England, 2001.
- [26]. R.N. Patel, A. Singh, K. K. Shukla, Y. Singh, *J. Coord. Chem.* 66 (2013) 4131.
- [27]. E. D. Broering, P. T. Truong, E. M. Gale, T.C. Harrop, *Biochemistry*, 52 (2013) 4.
- [28]. J. L. Wuerges, Y. I. Yim, H. S. Kang, K. G. Carugo, *Proc. Natl. Acad. Sci., USA*, 101 (2004) 8569.
- [29]. (a). J. S. Valentine, P. J. Hart, *Proc. Natl. Acad. Sci. USA*, 100 (2003) 3617.  
(b). **I.A. Abreu, D. E. Cabelli, *Biochem. Biophys. Acta*, 1804(2010) 263.**
- [30]. (a). S. Bharti, M. Choudhary, B. Mohan, S.P. Rawat, S.R. Sharma, K. Ahmad, *J. Mol. Struct.* 1149(2017)846.  
(b). **S. Bharti, M. Choudhary, B. Mohan, *J. Coord. Chem.* 71(2018)284.**
- [31]. (a). B. Shafaatian, Z. Ozbakzaei, B. Notash, S. A. Rezuani, *Spectrochim. Acta A*, 140 (2015) 248.  
(b). B. Shafaatian, A. Soleymanpour, N. Kholghioskouei, B. Notash, S. A. Rezuani, *Spectrochim. Acta A*, 128 (2014) 363.
- [32]. (a). **S. Fox, R. T. Stibrany, J.A. Potenza, S. Knapp, H. J. Schugar, *Inorg. Chem.* 39(2000)4950.**  
(b). **R. Uma, M. Palaniandavar, *Trans. Met. Chem.*, 18(1993)629.**  
(c). **W. M. Teles, M. V. Marinho, M. I. Yoshida, N. L. Speziali, K. Krambrock, C. B. Pinheiro, N.M. Pinhal, A. A. Leitao, F. C. Machado, *Inorg. Chim. Acta*, 359(2006)4613.**  
(d). **M. Palaniandavar, M. Sujatha, *Trans. Met. Chem.*, 19(1994)439.**  
(e). **G. Y. Kreitman, J. C. Danilewicz, D. W. Jeffery, R. J. Elias, *J. Agric. Food Chem.*, 65(2017)2564.**
- [33]. R. N. Patel, A. Singh, K. K. Shukla, D. K. Patel, V. P. Sondhiya, S. Dwivedi, *J. Sulfur Chem.* 31 (2010) 299.
- [34]. N. C. Kasusa, K. Sekino, M. Ishikawa, A. Honda, M. Yokoyama, S. Nakano, N. Shimada, C. Koumo, K. Nomiya, *J. Inorg. Biochem.* 96 (2003) 298.
- [35]. G. M. Sheldrick, *SADABS (Version 2.03)*, University of Gottingen, Germany, 2002.
- [36]. G. M. Sheldrick, *Acta Crystallogr. Sect. A*, 71(2015)3.
- [37]. M. C. Burla, R. Caliendo, B. Carozzini, G. L. Cascarano, C. Cuocci, C. Giacovazzo, M. Mallamo, M. Mazzone, G. Polidori, *J. Appl. Crystallogr.* 48(2015)306.
- [38]. L. J. Bourhis, O. V. Dolomunov, R. J. Gildea, J. A. K. Howard, H. Puschmann, *Acta Crystallogr. Sect. A*, 71(2015)59.
- [39]. G. R. Brubker, J.C. Latta, D. C. Aquino, *Inorg. Chem.* 9 (1970) 2608.
- [40]. E. C. Constable, C. E. Housecroft, J. A. Zambese, *Inorg. Chem. Commun.* 14 (2011) 1703.
- [41]. S. Dhar, M. Nethaji, A. R. Chakravarty, *Dalton Trans.* (2005) 344.

- [42]. E. Labisbal, J. Romero, A. Blas, J.A.G.-Vasquez, M. Duran, A. Sousa, *Polyhedron*, 11 (1992) 53.
- [43]. W. J. Geary, *Cord. Chem. Rev.* 78(1971)81.
- [44]. T.E. Gilchrist, *Heterocyclic Chemistry*, 2<sup>nd</sup> edn. Longman/Wiley, Harlow, Chi Chester (1992).
- [45]. (a). H. Xu, C. Luo, Z. Li, H. Xiang, X. Zhou, *J. Heterocyclic Chem.* 53 (2016) 1207.(b). S. Fox, R. T. Stibrany, J. A. Potenza, S. Knapp, H. J. Schugar, *Inorg. Chem.* 39(2000)4950.
- [46]. (a).M. Amini, M. Bagherzadeh, B. E. Sis, A. Ellern, L. K. Woo, *J. Coord. Chem.*66 (2013)1897. (b). M. Amini, A. Arab, R. Soleyman, A. Ellern, L. K. Woo, *J. Coord. Chem.*66 (2013)3770. (c). N.-Y. Jin, *J. Coord. Chem.*65 (2012)4013. (d). M. Bagherzadeh, M. Zare, *J. Coord. Chem.*66 (2013)2885. (e). B. Shafaatian, S. S. Mousavi, S. Afshari, *J. Mol. Struct.* 1123 (2016) 191.
- [47]. P. P. Netalkar, S. P. Netalkar, S. Budagumpi, V. K. Revankar, *Eur. J. Med. Chem.*, 79(2014)47.
- [48]. K. Nakamoto, *Infrared and Raman spectra of Inorganic Coordination Compounds, Part B-Application in Coordination, Organometallic and Bioinorganic chemistry*, John Wiley and sons, New York (2009).
- [49]. S. Durmus, A. Atahan, M. Zengin, *Spectrochim. Acta A*, 84 (2011) 1.
- [50]. S. Sarkar, K. Dey, *Spectrochim. Acta A*, 62 (2005) 383.
- [51].M. Kalita, K. J. Tamuli, P. Barman, B. Sharma, R. Baruah, H. P. D. Baruah, *Polyhedron* 97 (2015) 140.
- [52].N. Sheppard, *Trans. Faraday Soc.* 46 (1950) 429.A. Mukherjee, S. Dhar, M. Nethaji, A. R. Chakravarty, *Dalton Trans.* (2005)349.
- [53].T. Rosu, E. Pahantu, C. Maxim, R. Georgescu, N. Stainlca, A. Gylea, *Polyhedron* 30(2011)154.
- [54]. J. L. Pierre, P. Chautempts, S. Refaif, C. Beguin, A. E. Marzouki, G. Serratrice, E. Saint-Aman and P. Rey, *J. Am. Chem. Soc.*117( 1995)1965.
- [55]. M.R.P Kurup, B. Varghese, M. Sithambaresan, Sithambaresan, S. Krishnan, S.R.Sheeja, E. Suresh, *Polyhedron*, 30(2011)70.
- [56]. M. Kalita, P.Gogoi, P. Barman, B. Sharma, *J. Coord.Chem*,67(2014)2445.
- [57]. M. Gulcan, Y. Karatas, S.Isik, G. Ozturk, E.Akbas, E.Sahin, *J. Fluoresc.* 24(2014)1679.
- [58]. C. M. Liu, R.G. Xiong, X. Z. You, Y.Z. Liu, *Polyhedron*,15(1996) 4565.
- [59]. C.W. Young, J. C. Dewan, H.R. Lilental and S.J. Lippard, *J. Am. Chem. Soc.*100 (1978)7291.
- [60]. A. Taha, *Spectrochim. Acta*, 59A (2003) 1373.
- [61]. J. C. Almeida, I. M. Marzano, M. Pivatto, N. P. Lopes, A. M. D. C. Ferreira, F. R Pavan, I. C. Silva, E. C. Pereira-Maia, G. V. Poelhsitz, W. Guerra, *Inorg. Chim. Acta*, 446 (2016) 87.
- [62]. J. C. Almeida, D. A. Paixao, I. M. Marzano, J. Ellena, M. Pivatto, N. P. Lopes, A. M. D. C. Ferreira, E. C. Pereira-Maia, S. Guilardi, W. Guerra, *Polyhedron*, 89 (2015)1.
- [63]. B. J. Hathaway, D. E. Billing, *Coord. Chem. Rev.* 5(1970) 143.

- [64]. R.N. Patel, Y. P. Singh, Y. Singh, R. J. Butcher, J. P. Jasinski, *Polyhedron*, 129(2017)164.
- [65]. R. N. Patel, Y. P. Singh, Y. Singh, B. J. Butcher, *Polyhedron*, 104 (2016)116.
- [66].R.N. Patel, Y. P. Singh, Y. Singh, R. J. Butcher, M. Zeller, R.K. B. Singh, O. U. -Wang, *J. Mol. Struct.* 1136 (2017)157.
- [67].Y. P. Singh, R.N. Patel, Y. Singh, R. J. Butcher, P. K. Vishakarma, R.K. B. Singh, *Polyhedron*, 122 (2017) 1.
- [68].Y. P. Singh, R.N. Patel, Y. Singh, D. Choquesillo-Lazarte, R. J. Butcher, *Dalton Trans.*46 (2017) 2803.
- [69].U. Weser, L. M. Schubotz, E. Lengfelder, *J. Mol. Catal.* 13 (1981) 249.
- [70]. W. S. Terra, S. S. Ferretra, R. O. Costa, L. L. Mendes, R. W. A. Franco, A. J. Bortoluzzi, J. A. L.C. Resende, C. Fernandes, A. H. Jr., *Inorg. Chim. Acta*, 450 (2016) 353.
- [71]. Y. Li, Z.Y. Yang, J.C. Wu, *Eur. J. Med. Chem.* 45 (2010) 5692.
- [72]. J. Han, Y. Xing, C. Wang, P. Hou, F. Bai, X. Zhang, M. Ge, *J. Coord. Chem.* 62(2009)745.
- [73]. A. Battistoni, F. Pacello, A. P. Mazzetti, C. Capo, J. S. Kroll , P. R. Lengford, A. Sansone, G. Donnarumma, P. Valenti, G. Rotilo, *J. Biol. Chem.* 276(2001)30315.
- [74]. Z. R. Liao, X.F. Zheng, B. S. Luo, L.R. Shen, D.F.Li, H.L. Liu, W. Zhao, *Polyhedron*, 20 (2001) 2813.
- [75]. P. J. Hart, M. M. Balbirnie, N. L. Ogihara, A. M. Nersissian, M. S. Weiss, J. S. Valentine, D. Eisenberg, *Biochemistry*, 38(1999)2167.
- [76]. K. Nomiya, R. Noguchi, K. Ohsawa, K. Tsuda, M. Oda *J. Inorg. Biochem.* 78 (2000) 363.
- [77]. D. X. West, S. B. Padhe, P. B. Sonawane, *Struct. Bond.* 76 (1991) 1.
- [78]. N.C. Kasusa, K. Sekino, C. Koumo, N. Shimada, M. Ishikawa, K. Nomiya *J. Inorg. Biochem.* 84 (2001) 55.
- [79]. D. X. West, H. Gebremedhin, R. J. Butcher, J. P. Jasinski, a. E. Liberta, *Polyhedron* 12 (1993) 2489.
- [80]. E. Bermjo, R. Carballo, A. Castineiras, R. Dominguez, C.M-Mossmer, J. Strable, D. X. West, *Polyhedron*, 18 (1999) 3695.
- [81].N. Raman, A. Kulandaisamy, K. Jeyasubramanian, *Synth. React. Inorg. Met. Org. Chem.*31 (2001)1249.

**Table 1.** Crystal data and structure refinement of ligands (L<sup>1b</sup>), (L<sup>2a</sup>) and H<sub>2</sub>La.

	L <sup>1b</sup>	L <sup>2a</sup>	H <sub>2</sub> La
Empirical formula	C <sub>14</sub> H <sub>11</sub> N O S	C <sub>28</sub> H <sub>18</sub> N <sub>4</sub> S <sub>2</sub>	C <sub>26</sub> H <sub>14</sub> Br <sub>2</sub> N <sub>4</sub> O <sub>6</sub> S <sub>2</sub>
Formula weight	241.30	474.58	702.35
Temperature (K)	293(2)	296(2)	296(2)
Wavelength (Å)	0.71073 Å	0.71073 Å	0.71073 Å
Crystal system	Monoclinic	Monoclinic	Triclinic
Space group	P2 <sub>1</sub> /n	C/2c	P-1
Unit cell dimensions			
<i>a</i> (Å)	7.3276(6) Å	14.8849(18) Å	8.2685(12) Å
<i>b</i> (Å)	12.6798(11) Å	8.3000(9) Å	11.7305(16) Å
<i>c</i> (Å)	12.7253(11) Å	19.664(2) Å	14.4154(18) Å
$\alpha$ (°)	90	90	102.618(7)
$\beta$ (°)	96.484(2)°	100.625(9)	96.008(7)
$\gamma$ (°)	90	90	100.367(7)
Volume (Å <sup>3</sup> )	1174.78(17)	2387.7(5)	1327.0(3)
D <sub>calc.</sub> (Mg/m <sup>3</sup> )	1.364	1.320	1.758
Z	4	4	2
Absorption coefficient (mm <sup>-1</sup> )	0.256	0.247	3.262
<i>F</i> (000)	504	984	696
Crystal size (mm)	0.30 x 0.25 x 0.20	0.35 x 0.35 x 0.30	0.30 x 0.20 x 0.20
$\theta$ Range for data collection (°)	2.275 - 25.000	2.11 - 28.36	1.46 - 28.32
Limiting index	-8<= <i>h</i> <=8 -15<= <i>k</i> <=15 -15<= <i>l</i> <=15	-19<= <i>h</i> <=19 -10<= <i>k</i> <=11 -24<= <i>l</i> <=26	-10<= <i>h</i> <=10 -15<= <i>k</i> <=14 -18<= <i>l</i> <=19
Reflections collected/unique [ <i>R</i> <sub>int</sub> ]	12602/2071 [0.0288]	12426 / 2797 [0.0596]	10649 / 5951 [0.0253]
Completeness to $\theta$	25.00–100%	28.36- 93.5 %	28.32 - 90.1 %
Absorption correction	Semi-empirical from equivalents	Semi-empirical from equivalents	Semi-empirical from equivalents
Max. and min. transmission	0.7455 and 0.6844	0.9295 and 0.9185	0.5615 and 0.4411
Refinement method	Full-matrix least-squares	Full-matrix least-squares	Full-matrix least-squares
Data / restraints / parameters	2071 / 0 / 154	2797 / 0 / 159	5951 / 0 / 365
Goodness-of-fit on <i>F</i> <sup>2</sup>	1.089	1.112	0.836
Final <i>R</i> indices [ <i>I</i> >2 $\sigma$ ( <i>I</i> )]	<i>R</i> <sub>1</sub> = 0.0361, <i>wR</i> <sub>2</sub> =0.0887	<i>R</i> <sub>1</sub> = 0.0655, <i>wR</i> <sub>2</sub> = 0.1434	<i>R</i> <sub>1</sub> = 0.0497 <i>wR</i> <sub>2</sub> = 0.1316
<i>R</i> indices (all data)	<i>R</i> <sub>1</sub> = 0.0548, <i>wR</i> <sub>2</sub> = 0.1061	<i>R</i> <sub>1</sub> = 0.0982, <i>wR</i> <sub>2</sub> = 0.16651750	<i>R</i> <sub>1</sub> = 0.1138 <i>wR</i> <sub>2</sub> = 0.1750
Largest diff. peak and hole (e.Å <sup>-3</sup> )	0.198 and -0.191	0.692 and -0.334	0.887 and -0.881

Table 2. Selected bond lengths (Å) and angles (°) for (L<sup>1b</sup>), (L<sup>2a</sup>) and H<sub>2</sub>La.

<b>(L<sup>1b</sup>)</b>				
<i>Bond length</i>	C(7)-S(1)	1.752(2)	C(7)-N(1)	1.301(3)
	C(13)-O(2)	1.361(2)	C(7)-C(8)	1.471(3)
<i>Bond angles</i>	N(1)-C(7)-C(8)	121.45(18)	N(1)-C(7)-S(1)	115.23(16)
<b>(L<sup>2a</sup>)</b>				
<i>Bond length</i>	S(2)-S(2)#1	2.0349(15)	N(1)-C(7)	1.234(4)
	N(1)-C(6)	1.415(4)	C(14)-N(2)	1.133(5)
<i>Bond angles</i>	C(5)-S(2)-S(2)#1	104.74(10)	C(7)-N(1)-C(6)	122.7(3)
<b>H<sub>2</sub>La</b>				
<i>Bond length</i>	S(1)-S(2)	2.062(2)	C(7)-N(2)	1.289(6)
	C(5)-O(3)	1.305(6)	C(19)-N(3)	1.415(5)
<i>Bond angles</i>	C(18)-S(1)-S(2)	103.96(17)	C(9)-S(2)-S(1)	103.91(17)
	C(7)-N(2)-C(8)	124.8(4)	C(20)-N(3)-C(19)	124.0(4)

Symmetry transformations used to generate equivalent atoms: #1 -x+2, y, -z+1/2 (L<sup>2a</sup>).

Table 3. IR characteristic band frequencies (cm<sup>-1</sup>) of the Schiff base ligands and its metal complexes.

Ligands/ Compounds	$\nu(\text{C}=\text{N})$	$\nu(\text{C}-\text{O})$	$\nu(\text{C}=\text{C})$	$\nu(\text{O}-\text{H})$	$\nu(\text{M}-\text{N})$	$\nu(\text{M}-\text{O})$	C-H	C-S	Ar-H
<b>HL<sup>1</sup></b>	1581	1157	1484	-	-	-	2910	755	3051
<b>HL<sup>2</sup></b>	1627	-	1464	-	-	-	2812	753	3032
<b>H<sub>2</sub>L</b>	1597	1230	1482	3390	-	-	2855	750	3045
<b>1</b>	1624	1136	1460	-	576	482	2918	751	3047
<b>2</b>	1635	-	1572	-	547	466	2890	749	3045
<b>3</b>	1635	1222	1565	3385	552	485	2872	747	3029

Table 4. Superoxide dismutase activity of some copper (II)/nickel (II) complexes.

S. N.	Metal complexes	IC <sub>50</sub> ( $\mu\text{mol dm}^{-3}$ )	K <sub>MCCF</sub> × 10 <sup>4</sup> (ML <sup>-1</sup> ) <sup>-1</sup> S <sup>-1</sup>	Reference
1.	<b>1</b>	44	3.75	This work
2.	<b>2</b>	41	5.52	This work
3.	<b>3</b>	39	4.12	This work
4.	HL <sup>1</sup>	62	-	This work
5.	HL <sup>2</sup>	59	-	This work
6.	H <sub>2</sub> L	56	-	This work
7.	CuCl <sub>2</sub> .2H <sub>2</sub> O	0.910	-	[70]
8.	Cu, Zn- SOD <sup>a</sup>	0.15	-	[69]
9.	Cu, Zn- SOD <sup>b</sup>	0.03	-	[69]
10.	Cu, Zn- SOD <sup>c</sup>	0.0026	-	[70]
11.	Cu, Zn- SOD <sup>c</sup>	0.04	-	[70]
12.	Vc	852	-	[71]
13.	[Cu(L <sub>2</sub> )]	42	7.86	[30]
14.	[Cu(L <sub>2</sub> ).DMF	45	8.50	[30]
15.	[(L) Cu (μ-CH <sub>3</sub> COO) <sub>2</sub> Cu(L)]	8.26	9.50	[22]
16.	[(L) Cu (μ-NO <sub>3</sub> ) <sub>2</sub> Cu(L)]	26	12.79	[22]
17.	[Cu(HL) <sub>2</sub> ].(ClO <sub>4</sub> ) <sub>2</sub>	63	5.28	[66]
18.	[Ni (HL) <sub>2</sub> ].NO <sub>3</sub> . ClO <sub>4</sub> . 0.5H <sub>2</sub> O	106	3.14	[66]
19.	[Cu((μ-CH <sub>3</sub> COO) (L) <sub>2</sub> ).4H <sub>2</sub> O	37	8.99	[66]

<sup>a</sup>NBT assay in the presence of alkaline DMSO: the other species were evaluated in the xanthine/xanthine oxidase system.

<sup>b</sup>IC<sub>50</sub> was determined by employing xanthine/xanthine oxidase –mediated reduction of NBT.

<sup>c</sup>IC<sub>50</sub> was determined by measuring the inhibition of the photoreduction of NBT.

k<sub>MCCF</sub> were calculated by  $K = k_{\text{NBT}} \times [\text{NBT}] / \text{IC}_{50}$ ,  $k_{\text{NBT}}$  (pH 7.8) =  $5.94 \times 10^4 \text{ (M L}^{-1}\text{)}^{-1} \text{ s}^{-1}$  [73,74].

Table 5. Antibacterial activities of tridentate Schiff bases and its metal complexes **1-3**.

Complexes (mM)	Diameter of inhibition zone (in mm)		
	<i>Salmonella typhi</i>	<i>Streptococcus aureus</i>	<i>E. Coli</i>
<b>HL<sup>1</sup></b>			
10	5	0	7
20	14	9	17
30	16	18	19
<b>HL<sup>2</sup></b>			
10	10	7	12
20	13	10	15
30	15	14	19
<b>H<sub>2</sub>L</b>			
10	0	4	8
20	10	15	14
30	15	19	22
<b>1</b>			
10	11	8	12
20	14	15	22
30	28	24	32
<b>2</b>			
10	9	7	16
20	21	13	24
30	23	22	31
<b>3</b>			
10	13	9	18
20	14	16	25
30	31	21	33
Chloramphenicol			
30	30	25	35
DMSO	None	None	None

Note: Key to interpretation (10-30mM): less than 10mm, inactive; 10-15mm, moderately active; above 15mm, highly active. DMSO (control) shows not clear inhibition zone. **Estimated error: ±1mM.**

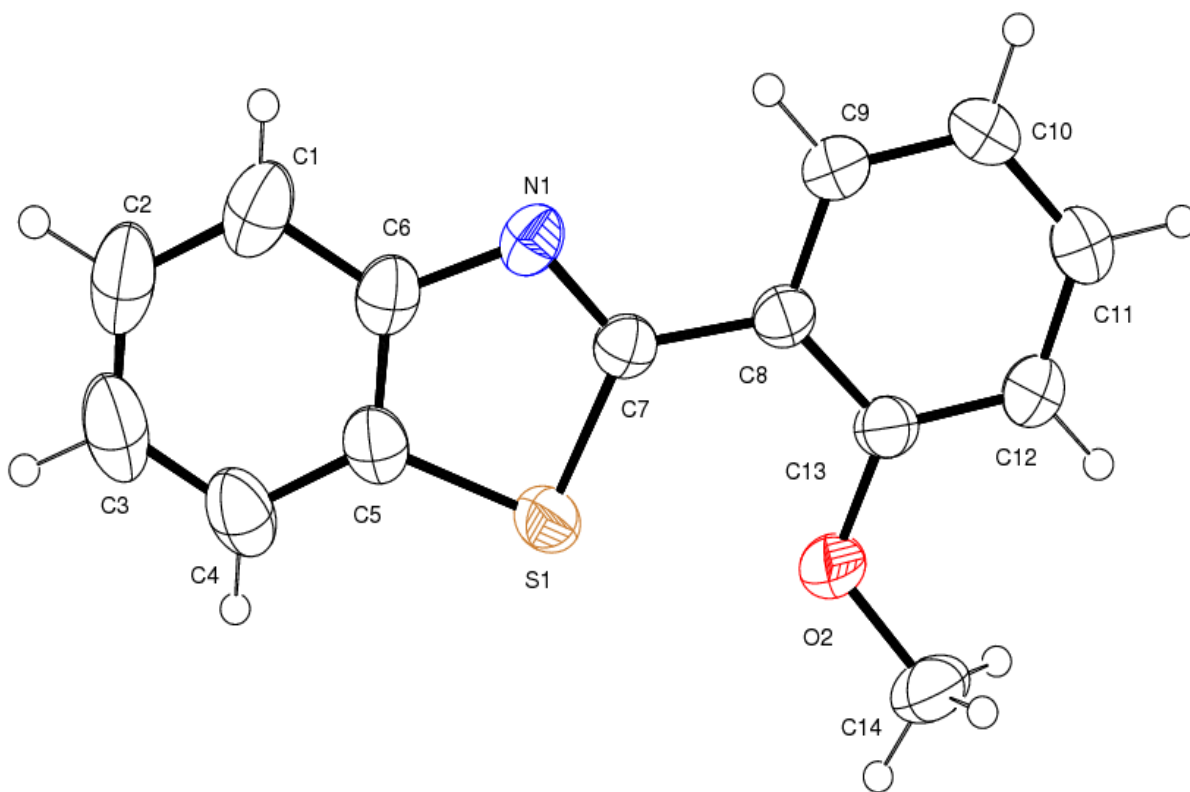


**Fig.1.** ORTEP structure of Schiff base (L<sup>1</sup>b) with 30% thermal ellipsoid and with atom numbering scheme.

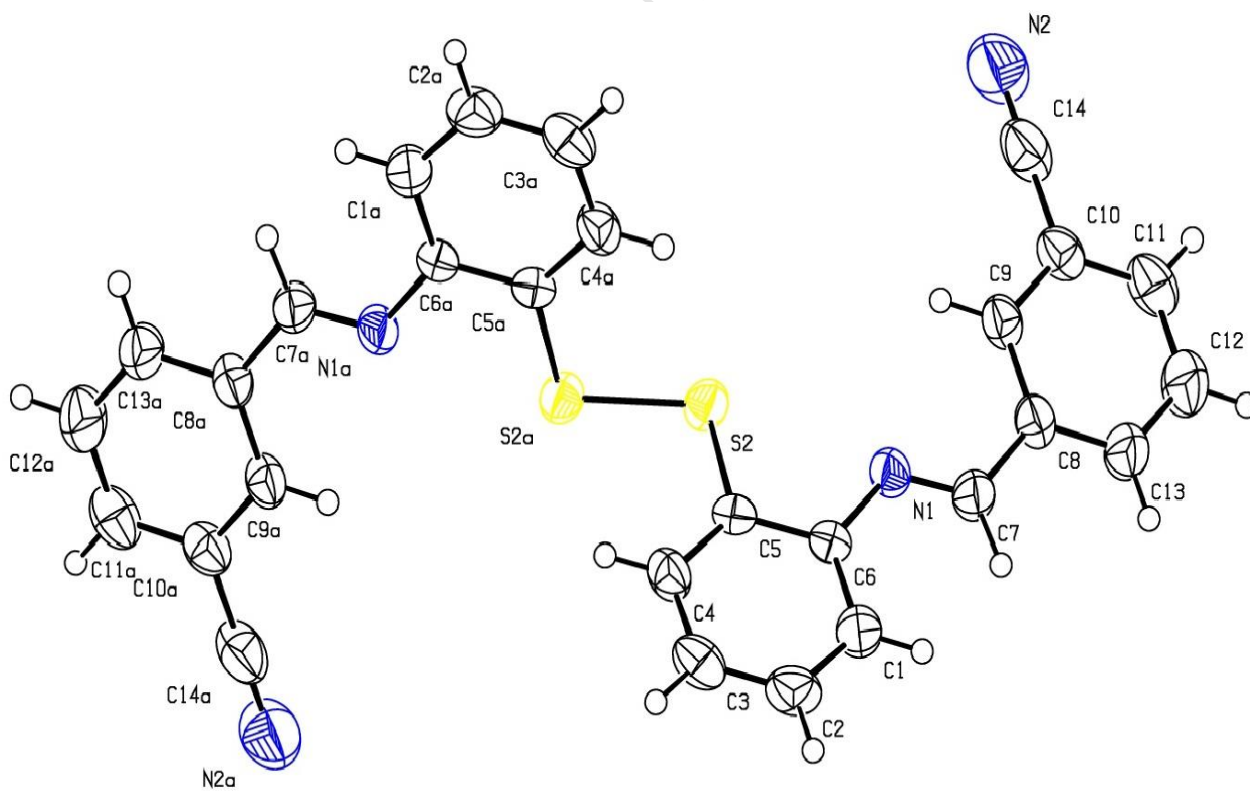


**Fig.2.** ORTEP structure of double Schiff base L<sup>2</sup>a with 50% thermal ellipsoid and with atom numbering scheme.

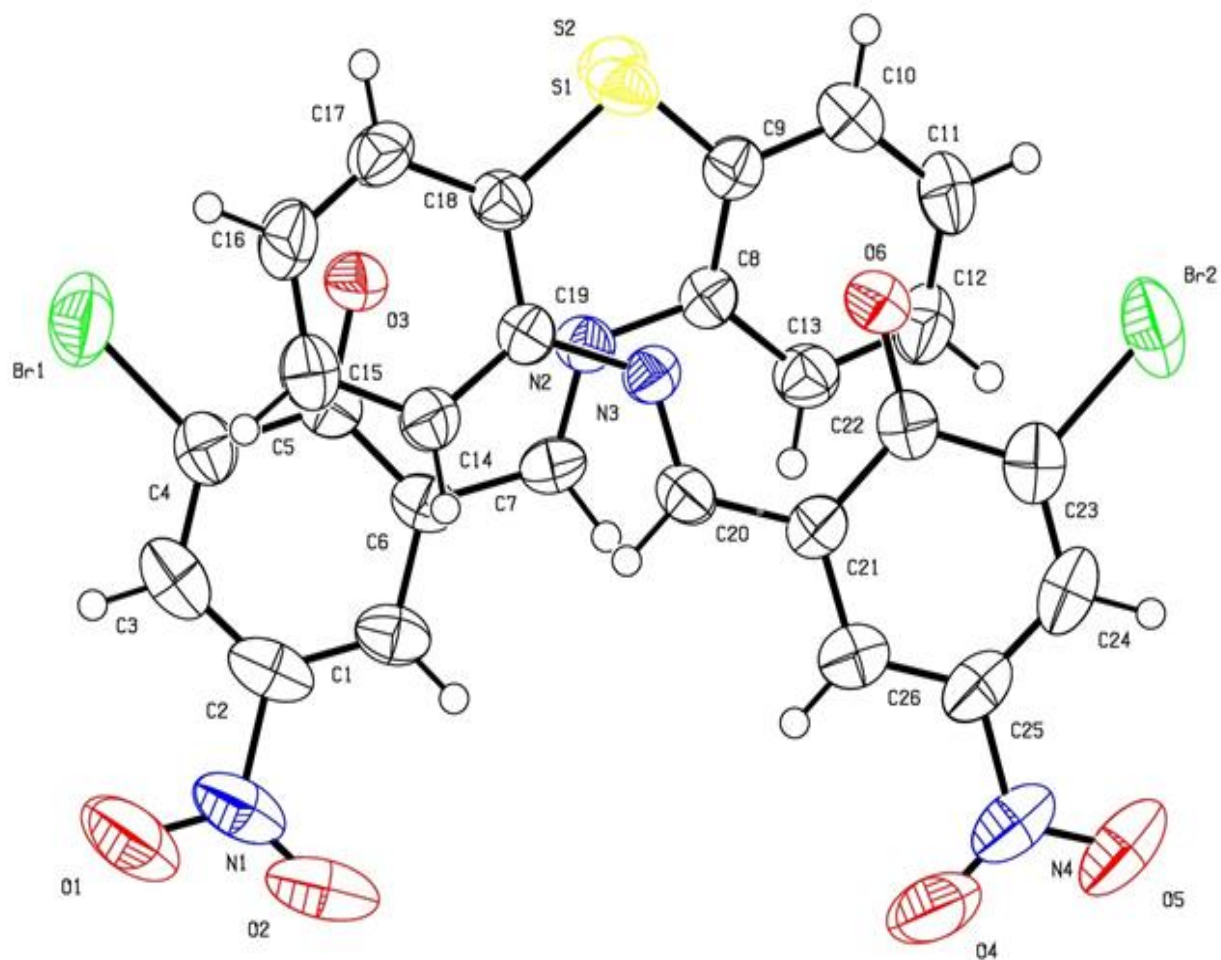


**Fig.3.** ORTEP structure of double Schiff base H<sub>2</sub>La with 50% thermal ellipsoid and with atom numbering scheme.

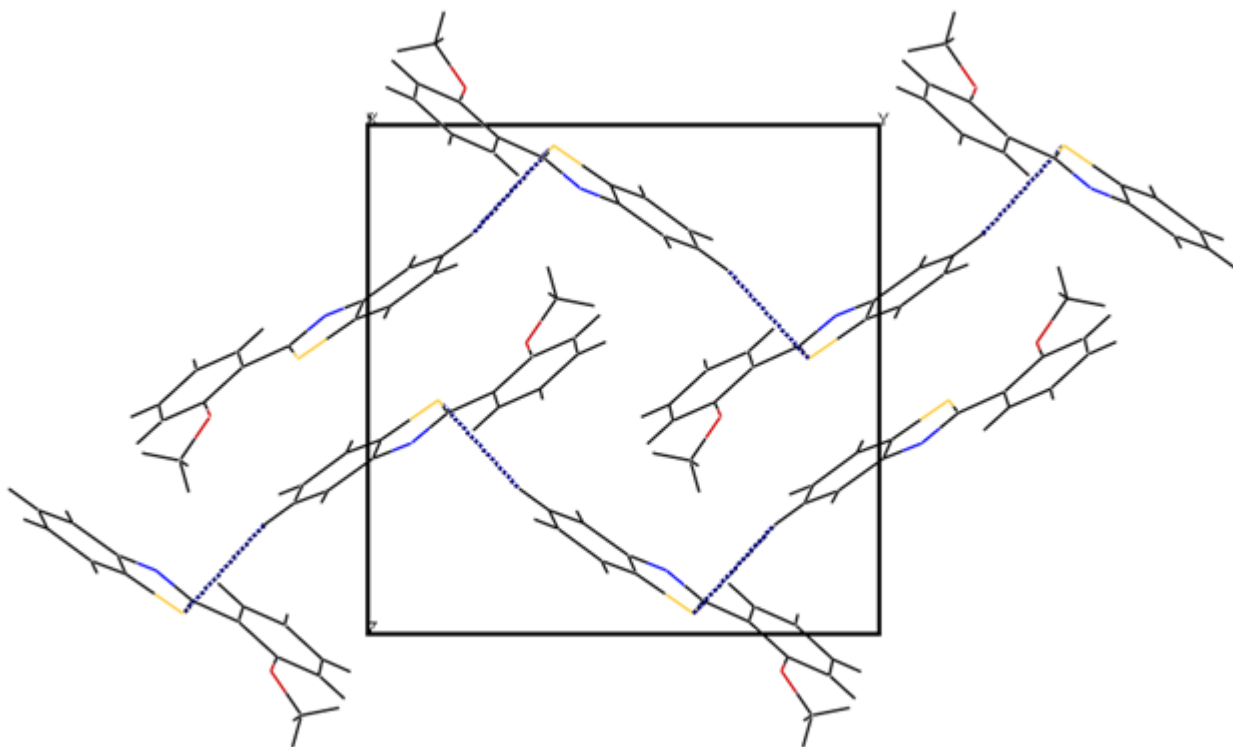


Fig.4. Perspective view of cell packing of Schiff base L<sup>1</sup>b along a-axis.

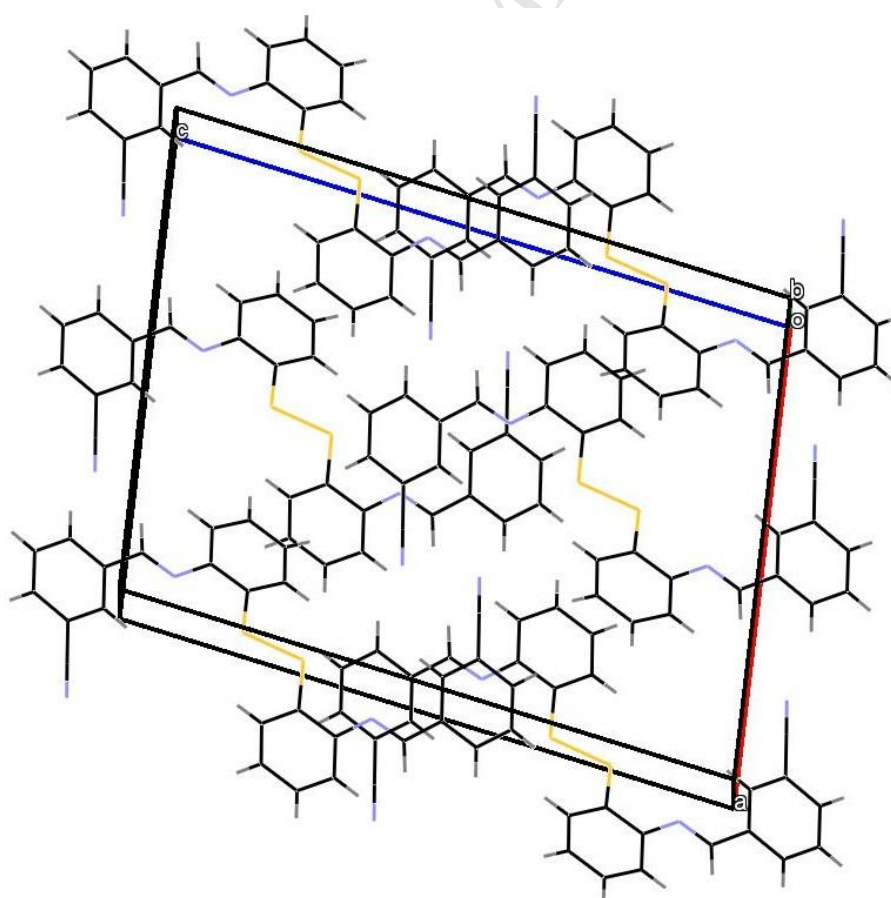
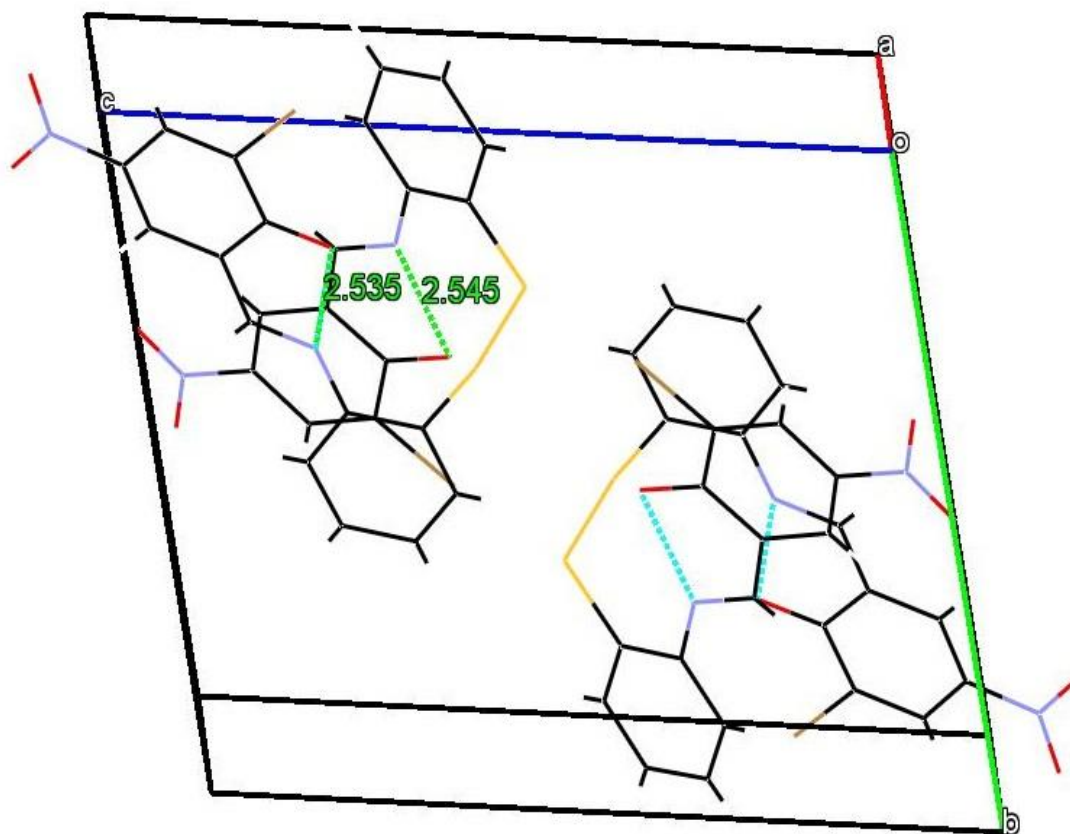
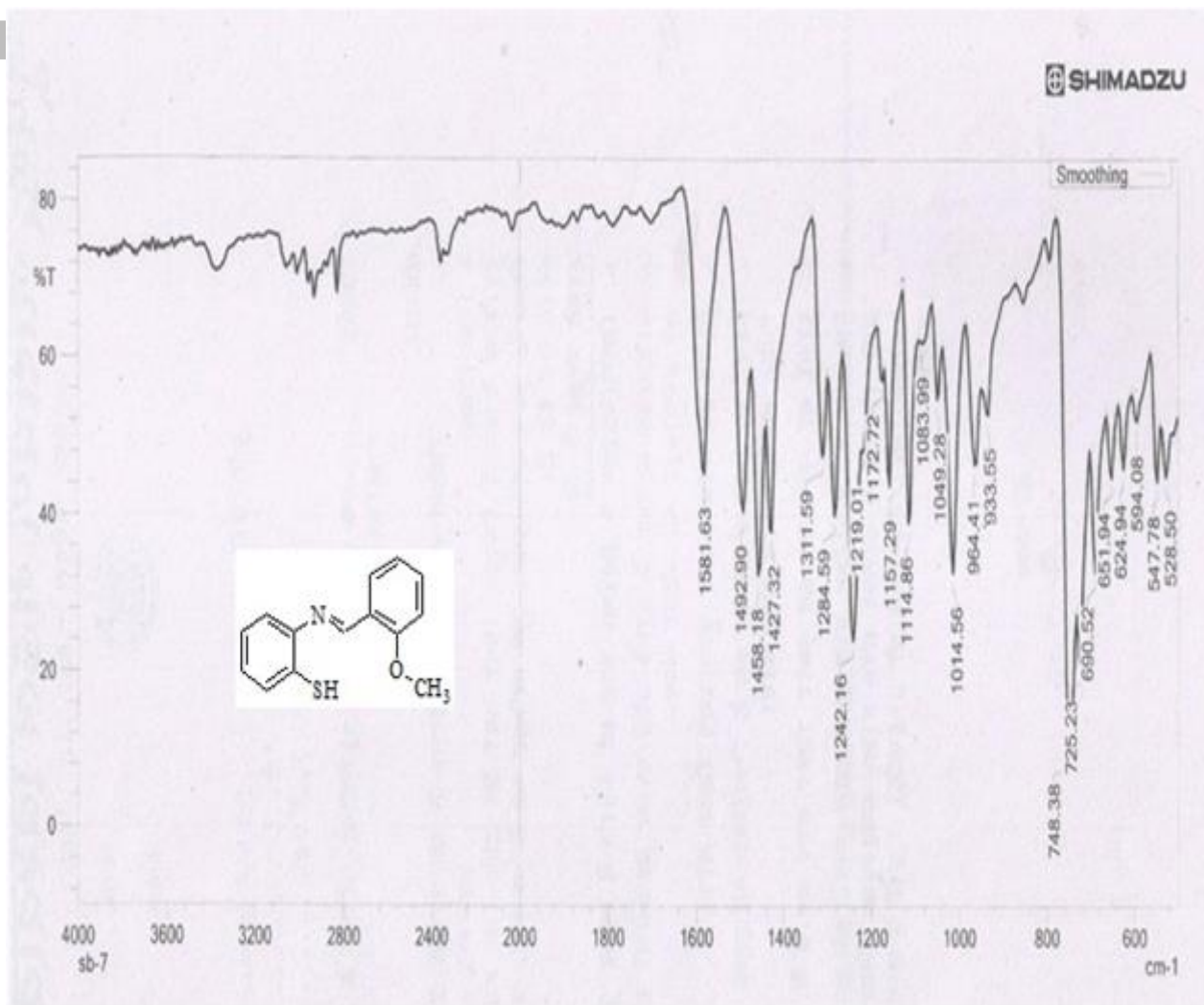


Fig.5. Perspective view of cell packing of Schiff base HL<sup>1</sup>a along a-axis.



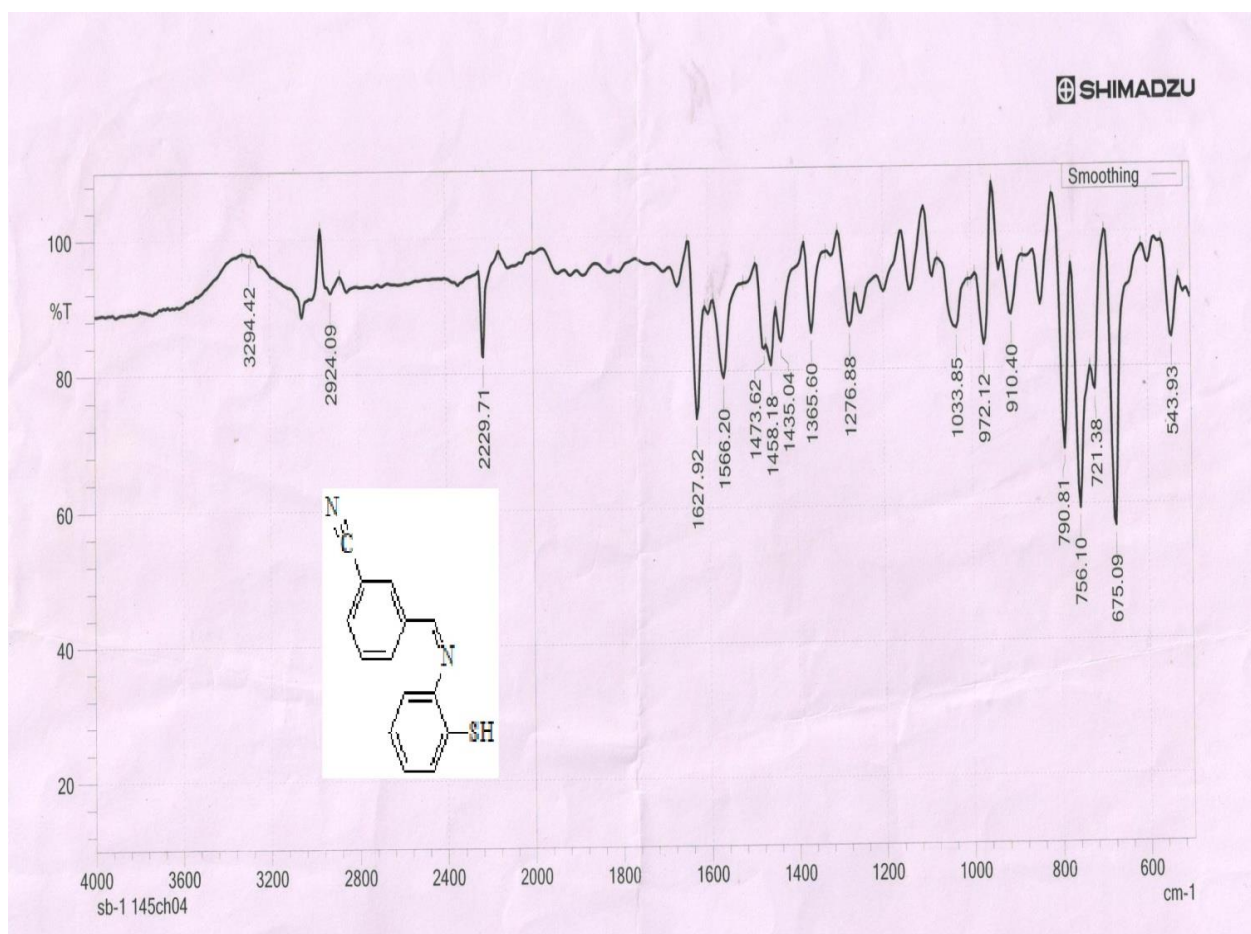
**Fig.6.** Perspective view of cell packing of Schiff base H<sub>2</sub>La along a-axis.

ACCEPTED



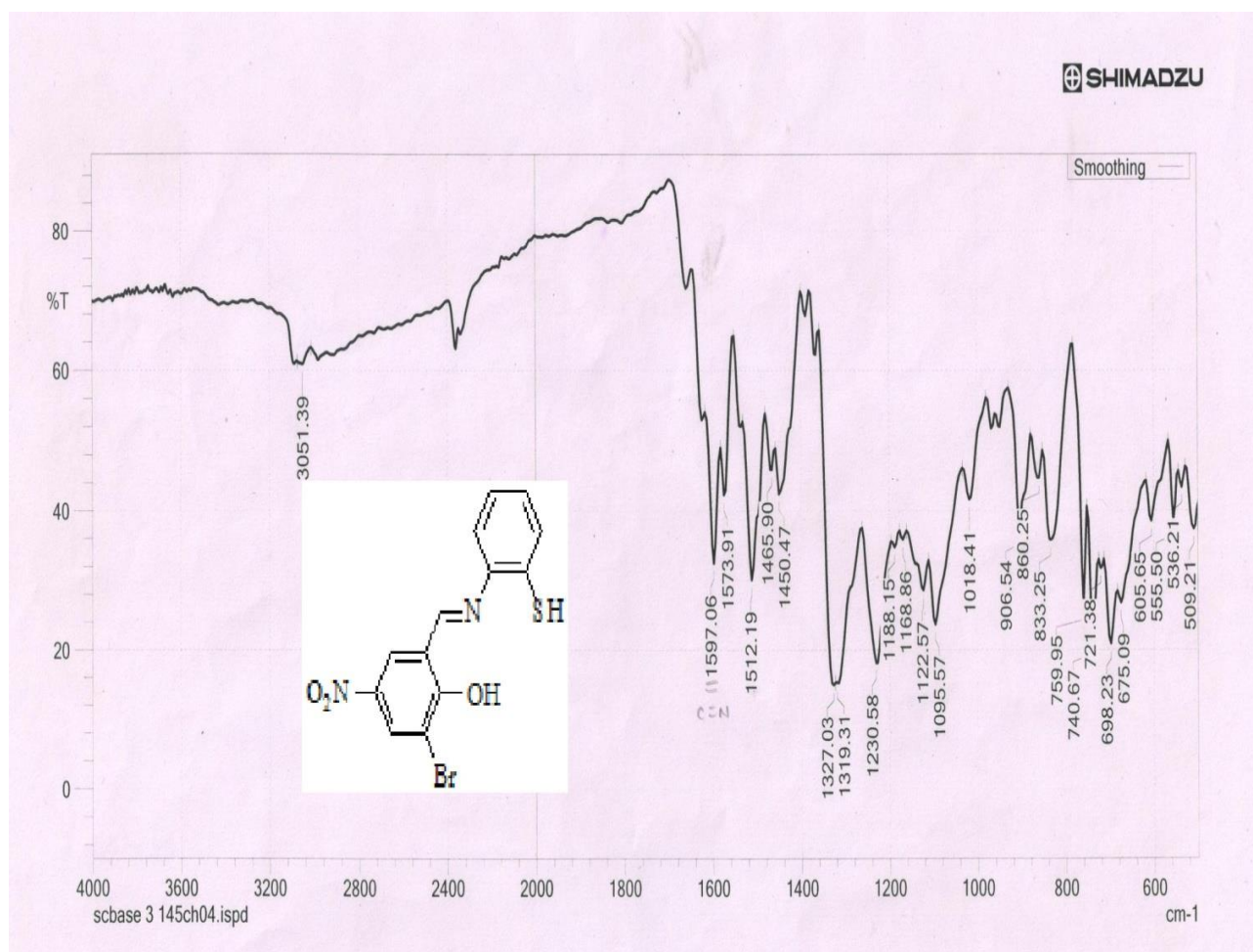
Wavenumber →

Fig.7. IR spectrum of tridentate Schiff base **HL<sup>1</sup>** ligand .



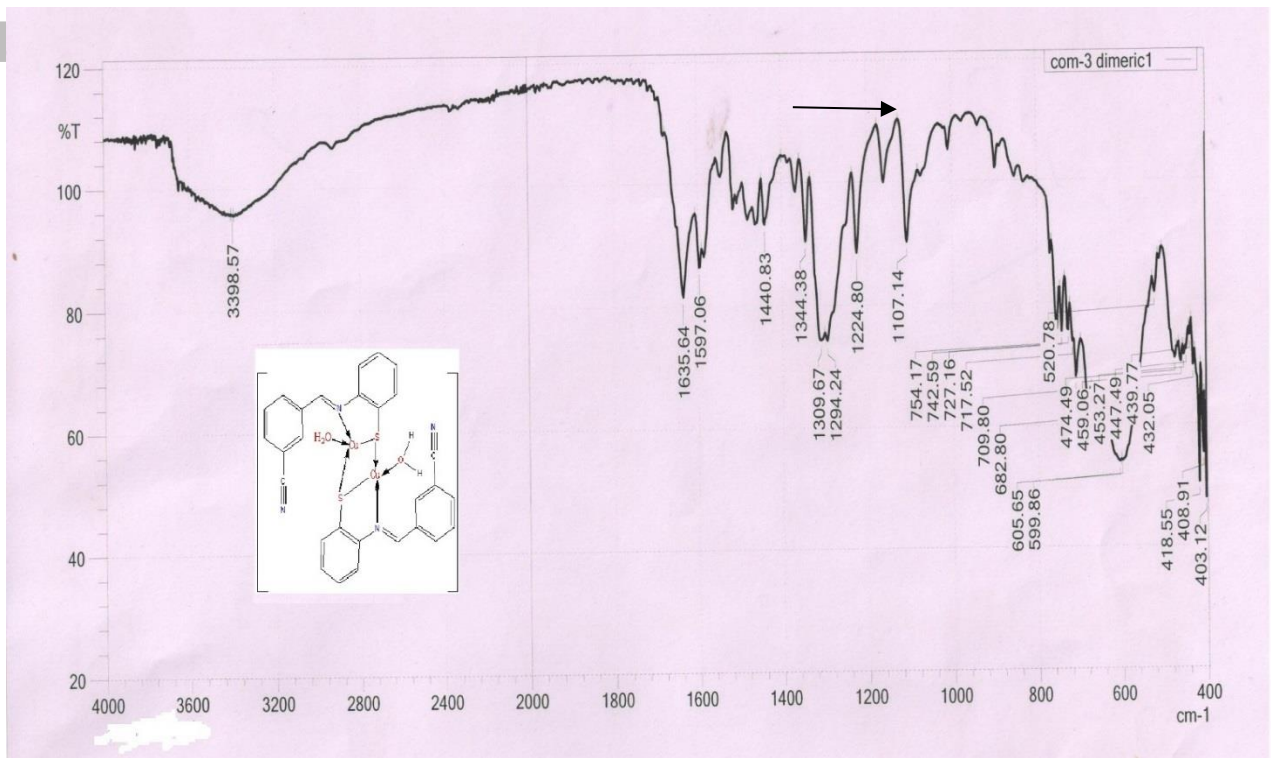
Wavenumber  $\longrightarrow$

Fig.8. IR spectrum of Schiff base  $HL^2$  ligand.



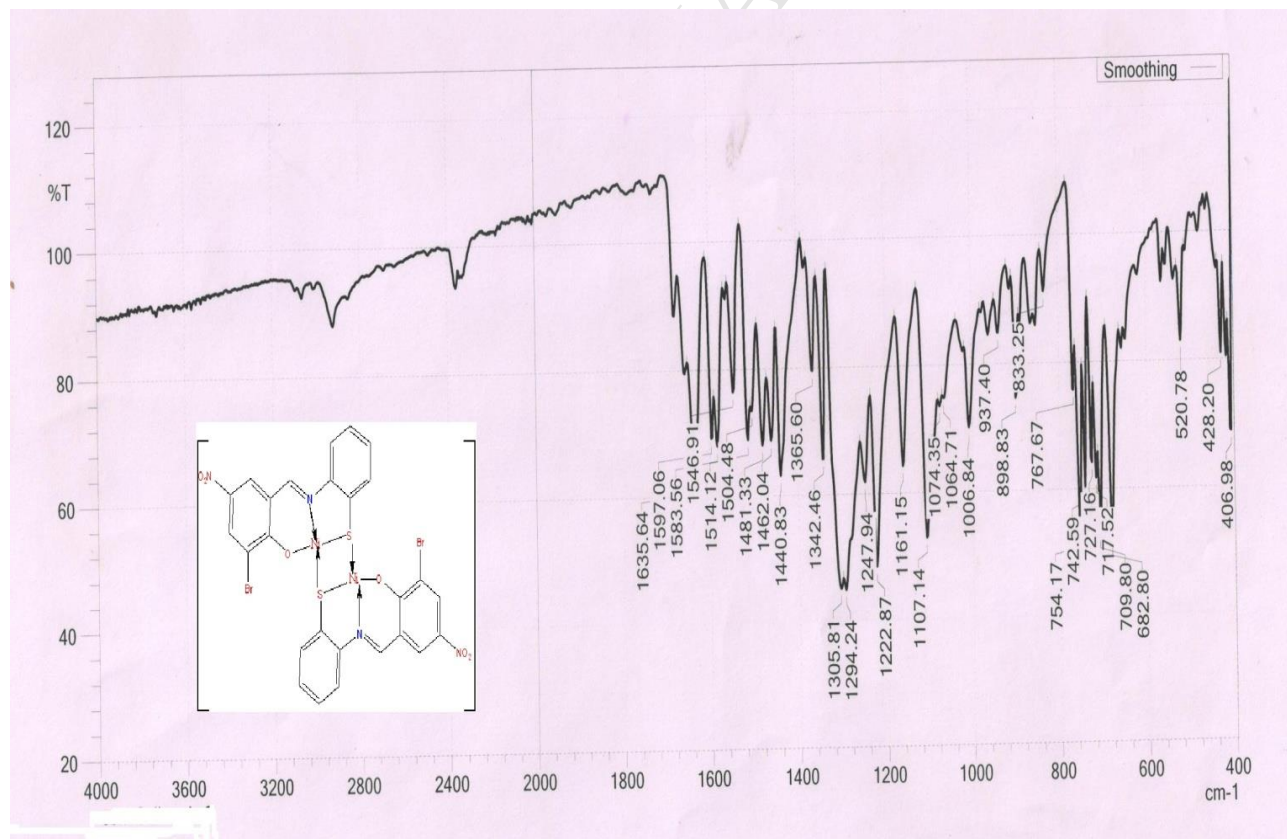
Wavenumber →

Fig.9. IR spectrum of Schiff base **H<sub>2</sub>L**.



Wavenumber

Fig. 10. IR spectrum of metallic complex 2.



Wavenumber →

Fig. 11. IR spectrum of metallic complex 3.

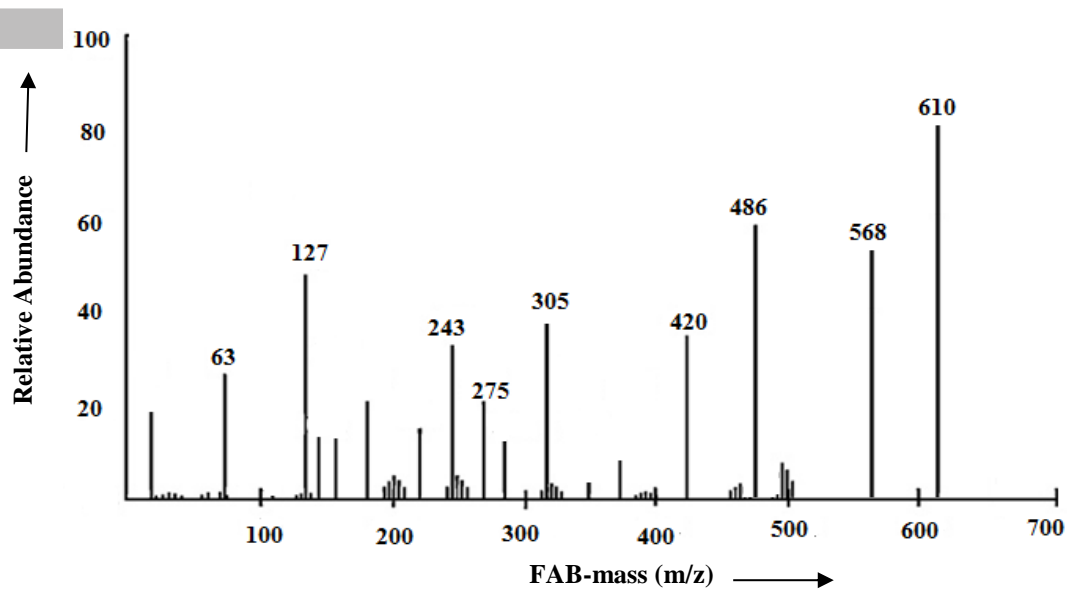


Fig. 12. FAB-mass spectrum of metallic complex 1.

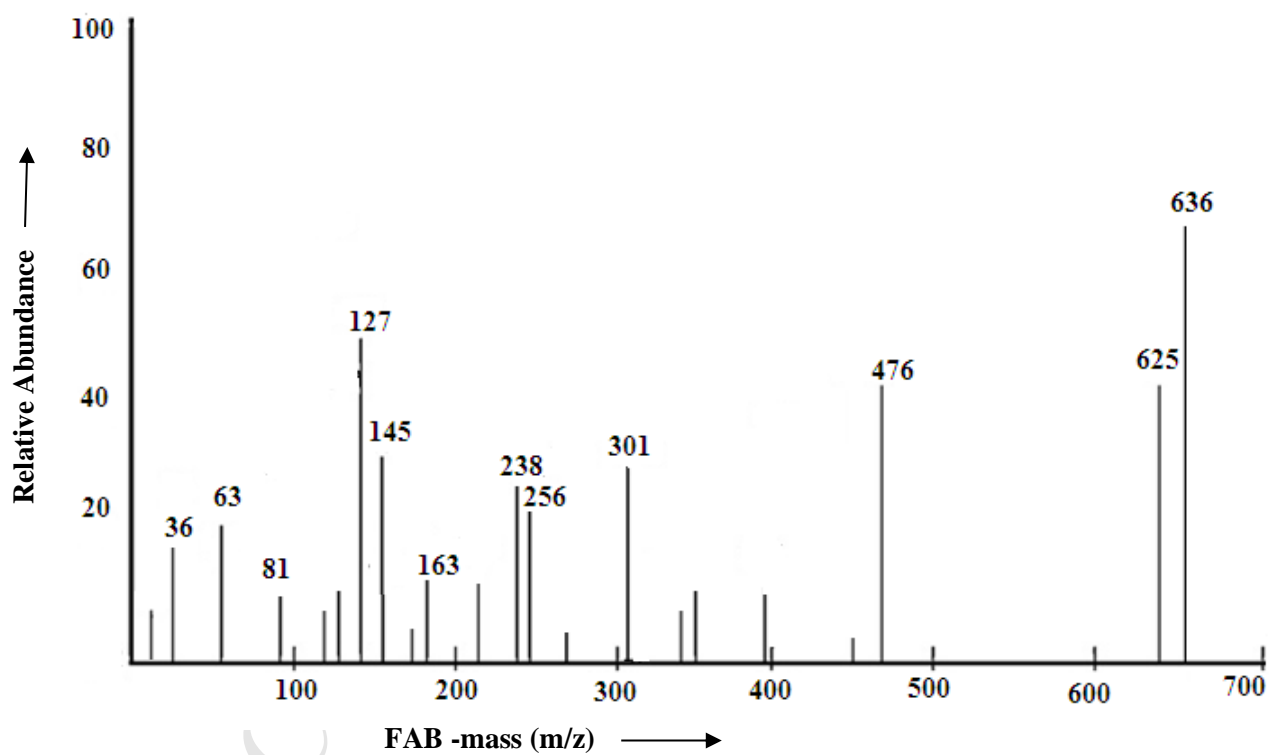
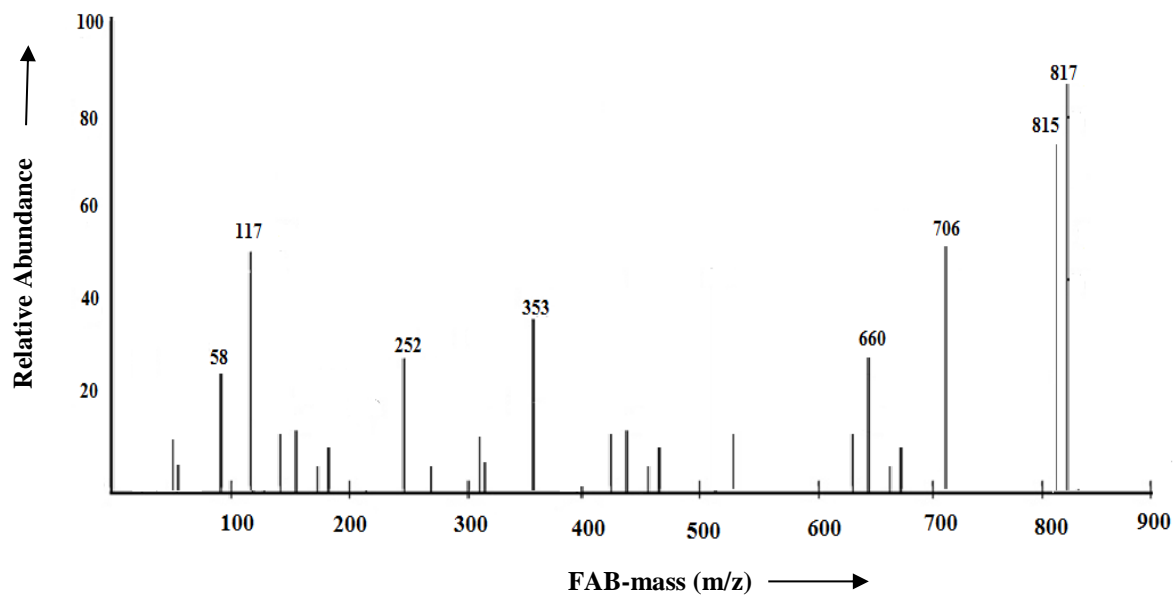
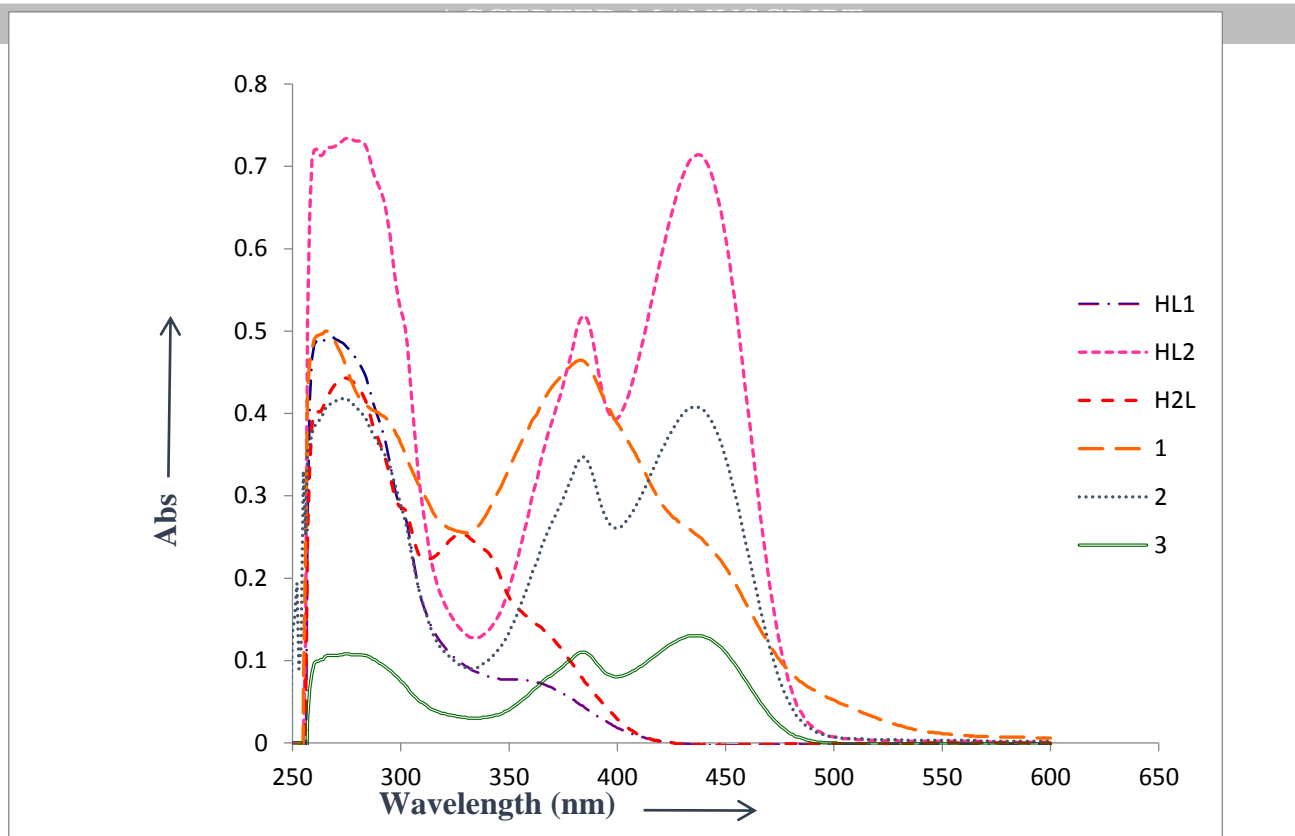


Fig. 13. FAB-mass spectrum of metallic complex 2.



**Fig. 14.** FAB-mass spectrum of **metallic complex 3**.



**Fig.15.** UV-Vis spectra ( $1 \times 10^{-5} \text{M}$ ) of the Schiff bases and their dimer complexes.

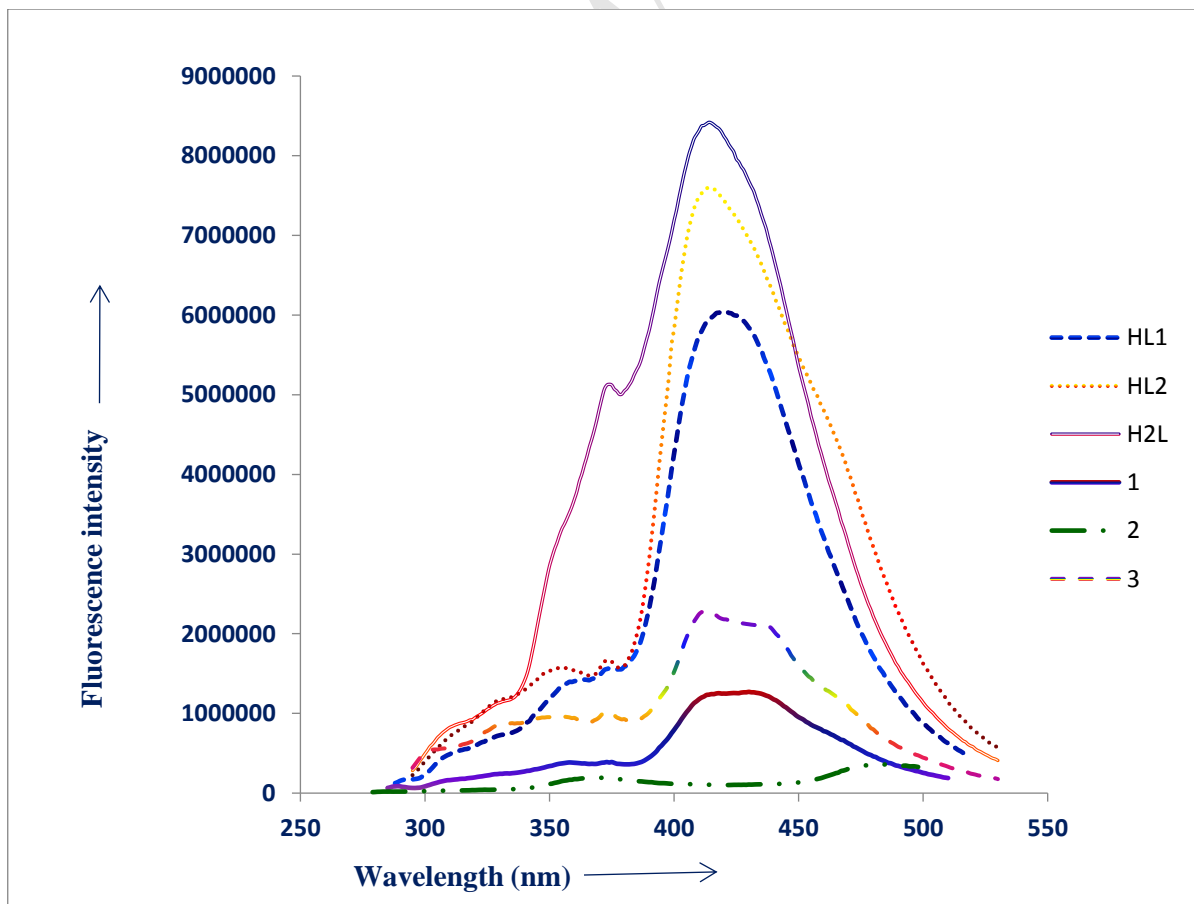


**Fig.16.** Emission spectra ( $1 \times 10^{-5} \text{M}$ ) of the Schiff bases and their dimer complexes.

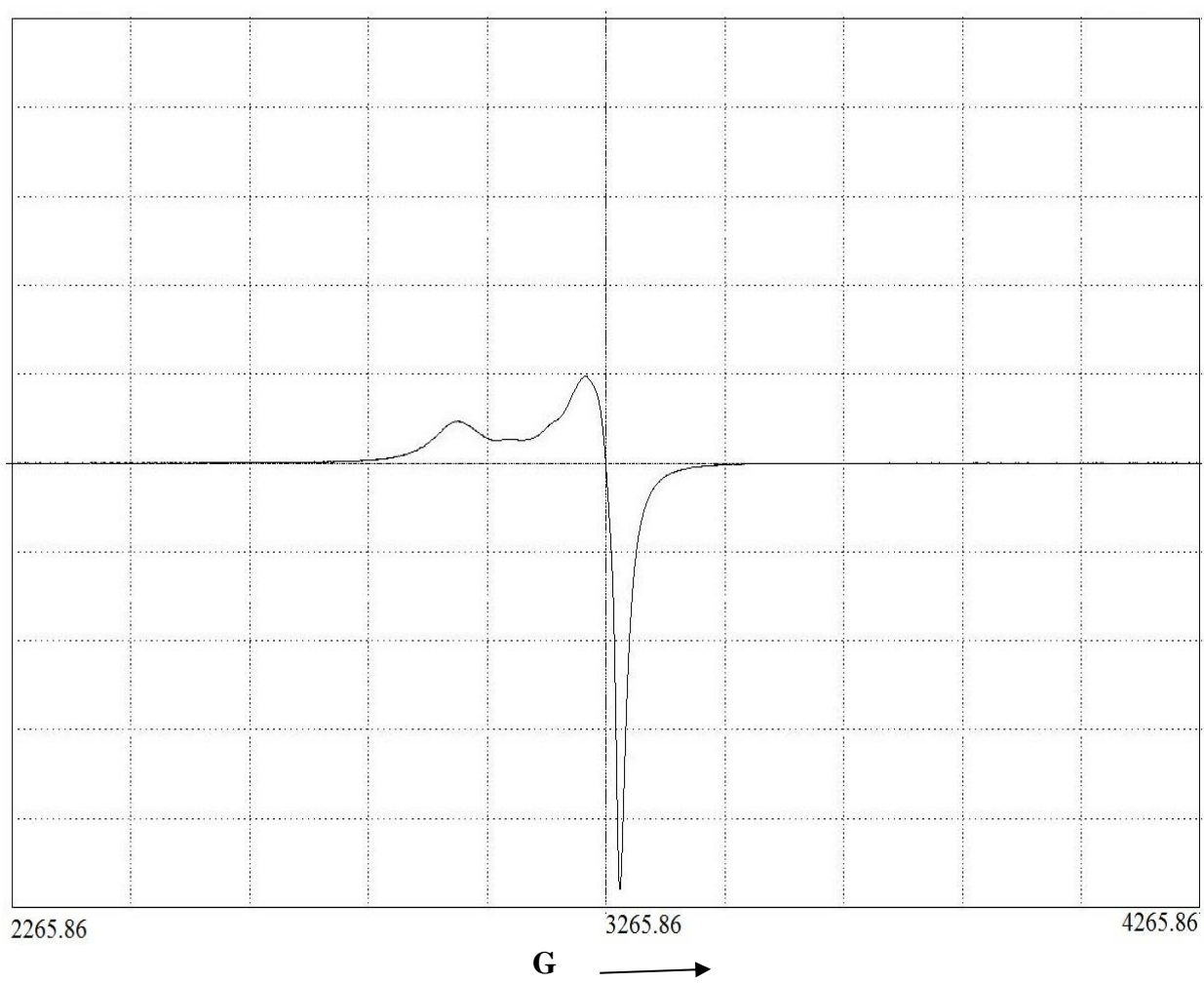


**Fig.17.** ESR spectrum (RT) in 100% DMSO of the copper complex **1**.

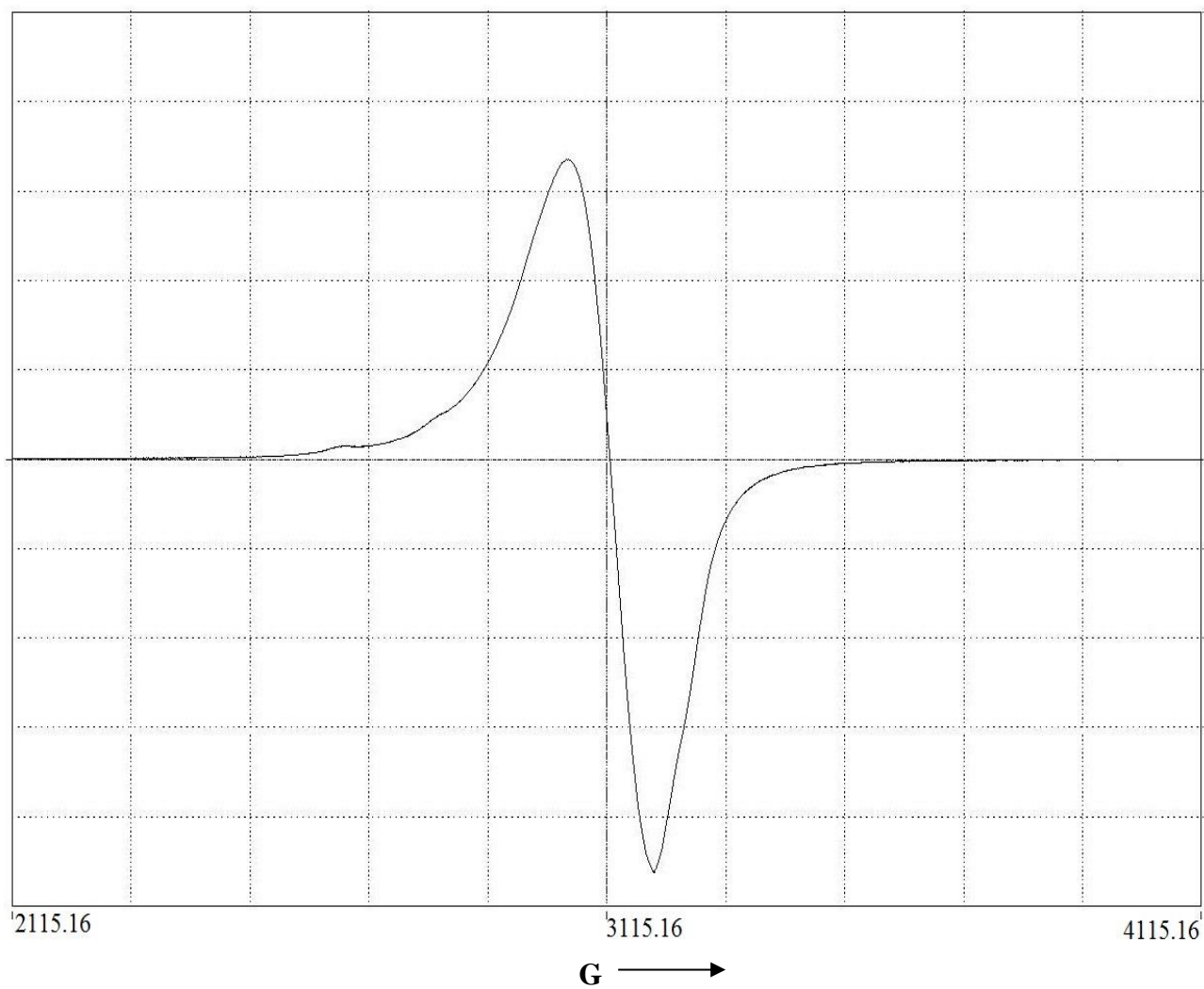


**Fig.18.** ESR spectrum (RT) in 100% DMSO of the copper complex **2**.

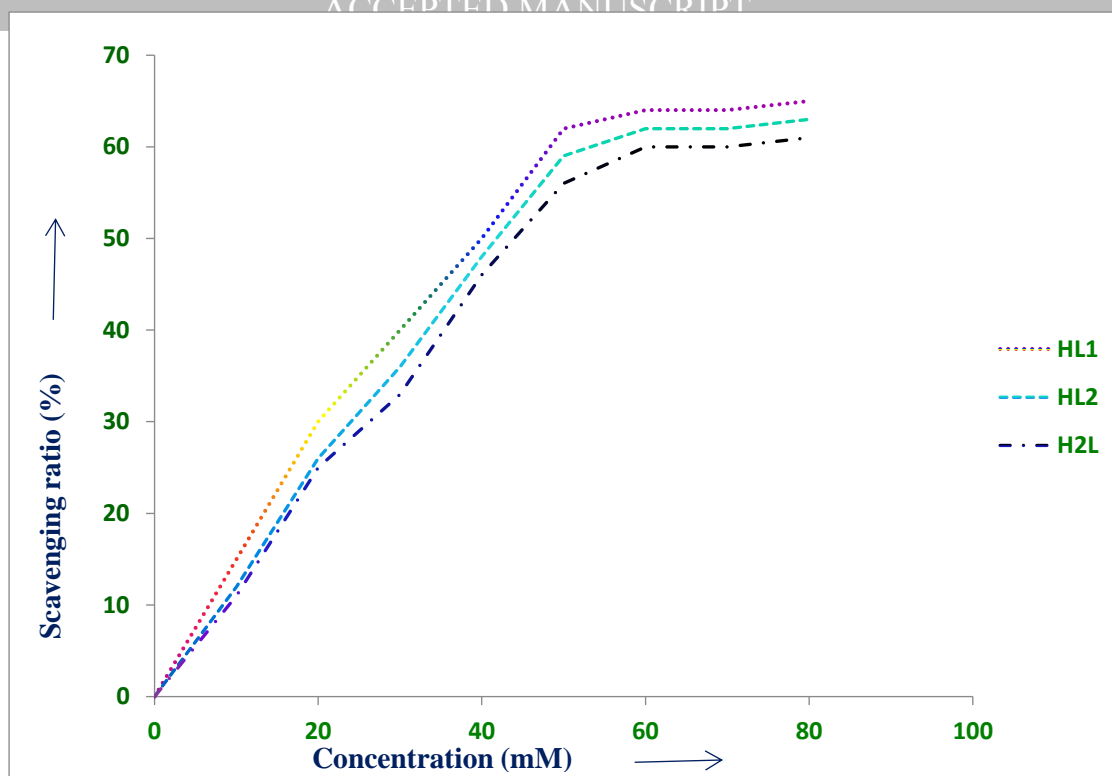


**Fig. 19.** SOD-like activities of the Schiff bases.

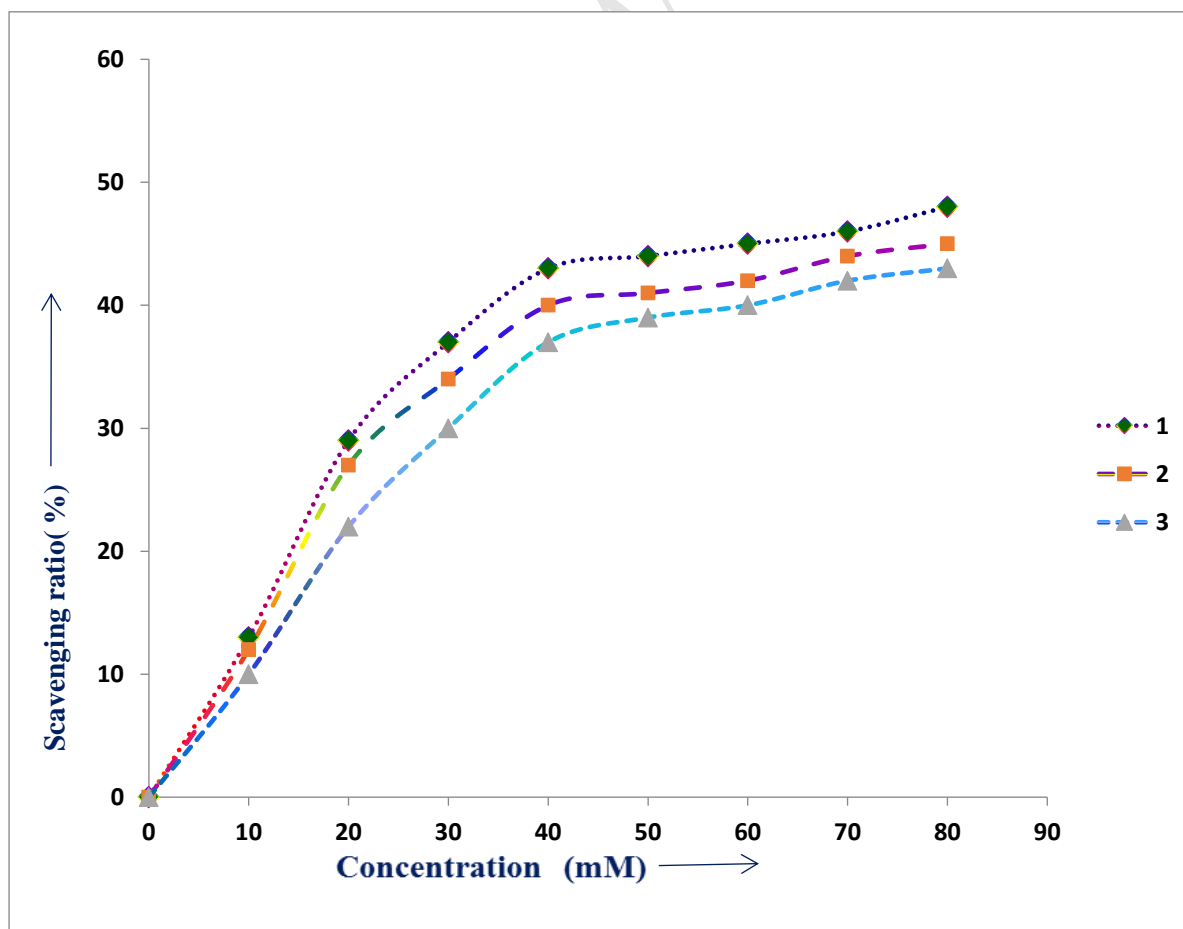


**Fig. 20.** SOD-like activities of dimer complexes 1-3.

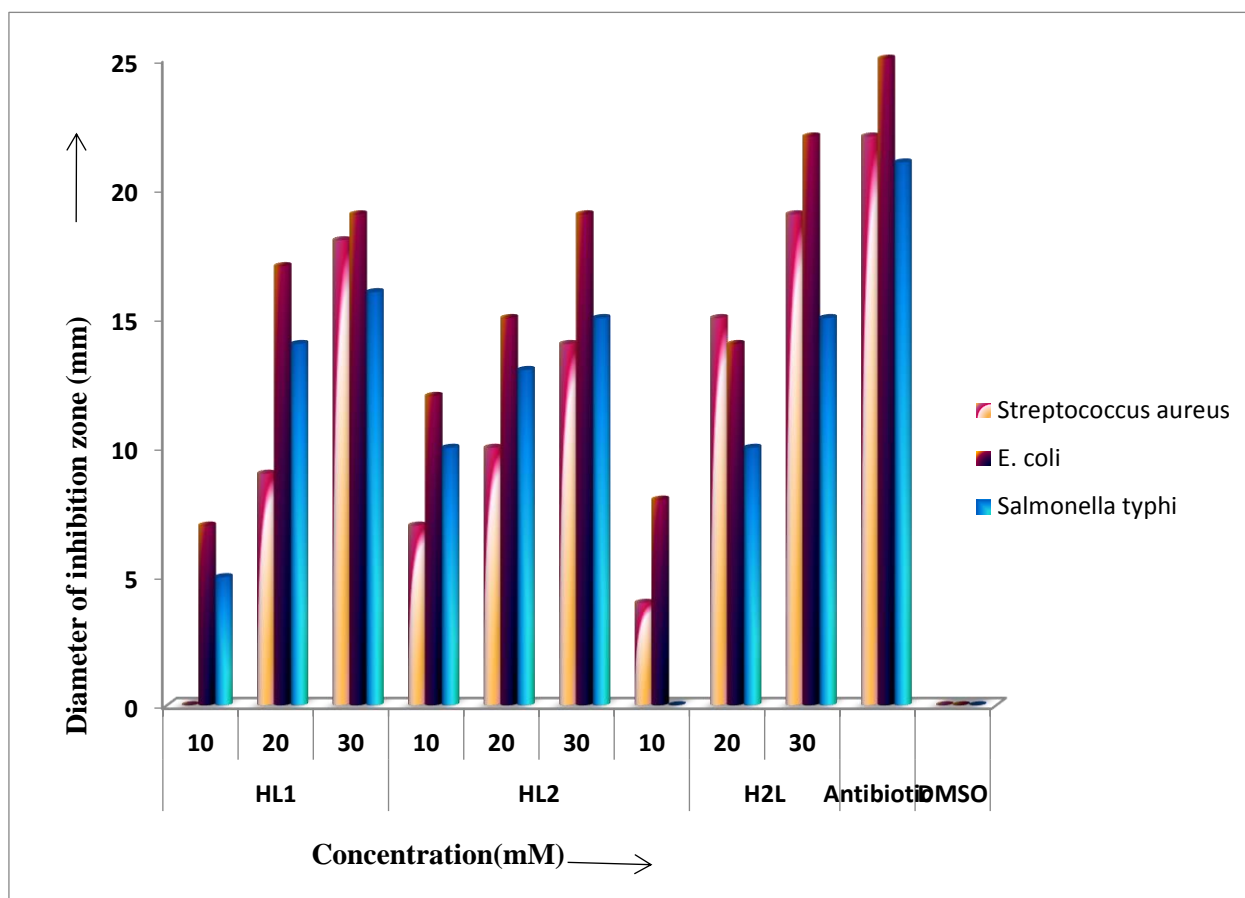


**Fig.21.**Antibacterial activity of the Schiff bases.

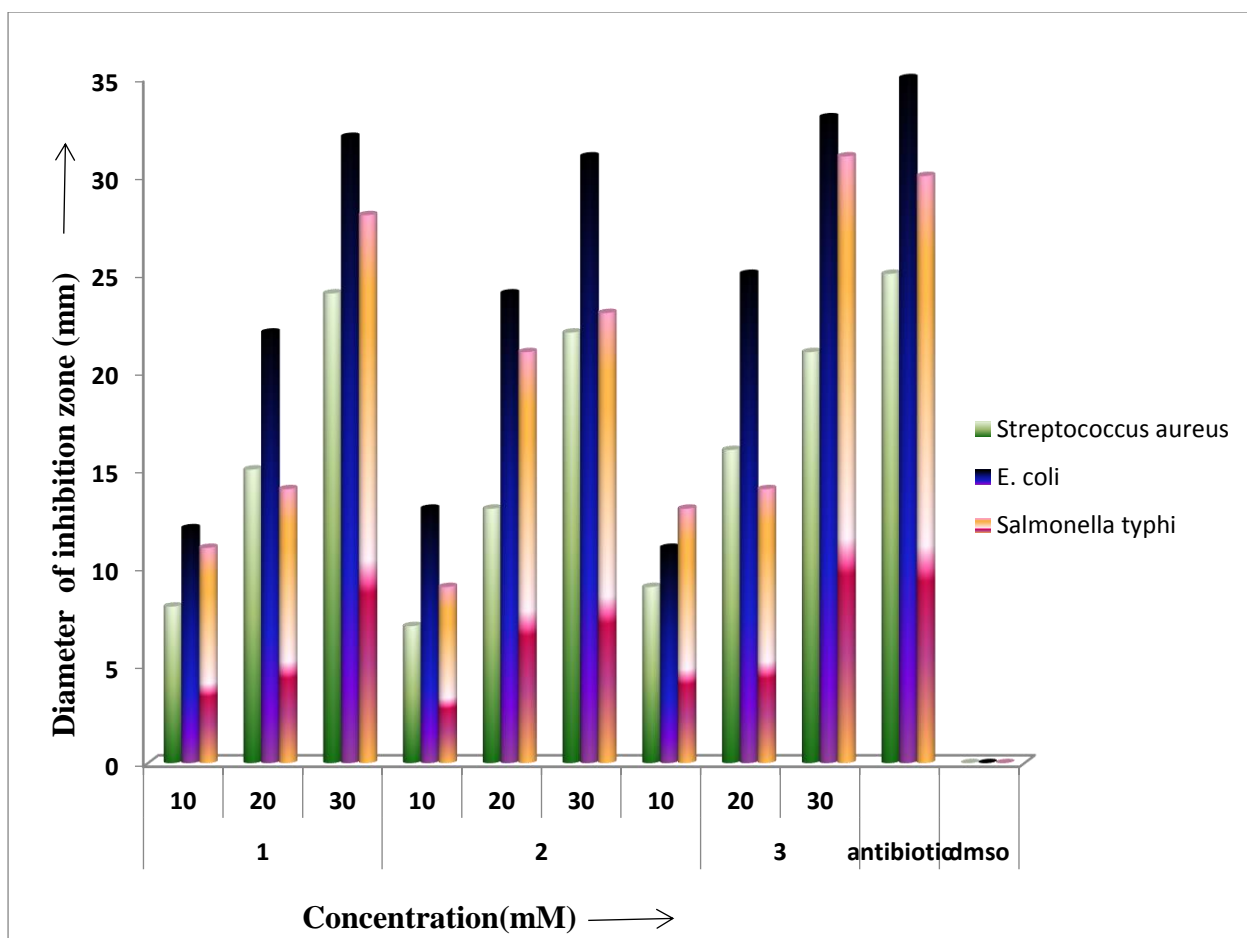


**Fig.22.** Antibacterial activity of the complexes 1-3.

**Highlights**

- **Design, syntheses and characterization of** dimer copper (II) and nickel (II) complexes containing 2-aminothiophenol moiety.
- Single crystal X-ray analyses determination of disulfide Schiff bases.
- **ESR**, FT-IR and UV-Vis spectroscopy.
- Catalytic activity of SOD-like metallic complexes.
- Antibacterial activity.